

## Materials and Methods

### ***Data availability***

The large-scale Cell Painting datasets used in this paper are publicly available and their details and locations are described in publications (gene overexpression dataset<sup>14</sup> and compound dataset<sup>15</sup>). RNA-sequencing data have been deposited into the NCBI Gene Expression Omnibus (GEO; accession number pending).

### ***Code availability***

The code used in this study is available at <https://github.com/broadinstitute/GeneCompoundImaging>. It is available for use under the BSD 3-clause license, a permissive open-source license.

### ***Cell line and DNA construct availability***

Cell lines and DNA constructs are available from the laboratories that performed the experiments using them, or where restricted by licensing, from commercial sources.

### ***Research animals***

*Boerckel lab*: Mouse experiments were conducted in compliance with all relevant regulations. All animal experiments were performed at the University of Pennsylvania under IACUC review and in compliance with IACUC protocol #806482.

### ***Feature set alignment***

As each experiment was analyzed by a slightly different CellProfiler pipeline, and also the phenotype of the negative controls are quite different (Figure 1b), an extra data preprocessing step is needed to make the feature sets comparable. To achieve this, we first took the intersection of features in the two datasets, which resulted in 605 features (1399 features in the genetic screen, without any feature selection; and 729 features in the compound screen, obtained using the findCorrelation with threshold of 0.90 on the original 1,783 dimensional feature set). In order to compare values of the corresponding features across experiments, each feature is standardized (mean-centered and scaled by standard deviation) with respect to the negative control. This was done platewise based on the mean and standard deviation of the controls at profile level for the compound dataset. The normalization parameters are slightly different for the genetic screen, where median and median absolute deviation (MAD) are used instead, to remove the outlier effects<sup>14</sup>. The code repository for all the analyses are publicly available as described in Code Availability.

### ***Scoring gene-compound connections***

We use Pearson correlation on aligned profiles of a gene and compound to score their connection. The profiles are obtained by averaging the replicate profiles feature-wise. We empirically found that an absolute score value greater than 0.35 indicates similar/opposite phenotypes in the gene and compound and used this for validation experiments. For the follow-up experiments of a gene, unless otherwise noted, we used a more stringent filter of 0.40 and picked the top 15 bioactive compounds that are positively correlated to the gene profile, and also 15 most negatively correlated ones. For the diversity-oriented-synthesis compounds in the set which are much less studied, we do the same, except that the top 30 in both directions are picked.

### ***Compound annotations***

Compound MOAs and target annotations were mainly acquired from the “Repurposing hub”<sup>49</sup> and then curated to include missing annotations from other sources, such as DrugBank<sup>50</sup>. This results in 747 compounds annotated with the gene(s) that they target. The protein interaction data, which was used to assess relevance of a protein to compound targets, was collected from BioGRID<sup>51</sup>.

### ***Enrichment p-value estimation***

We estimate the p-values of candidate compound list enrichment empirically, by counting the number of valid connections in the list, and ranking it against a null distribution. The null distribution is defined as the same count for random lists of the same size as the original list, and is sampled many times. The p-value estimation is repeated many times and the final estimation is obtained by averaging the individual estimates.

### ***Enrichment Analysis Plot***

We follow the same logic as the Gene Set Enrichment Analysis (GSEA)<sup>52</sup>. The set of gene-compound pairs are sorted based on their profile correlations on the x-axis. On the y-axis, the plot goes up by a certain fixed amount if the corresponding gene-compound is a valid pair. Otherwise, the plot goes down by the same fixed amount. Scanning the x-axis from left to right, early existence of abundant valid pairs results in a rapid jump of the plot, and illustrates higher enrichment of profile correlation for being indicative of biological relevance between the gene-compound pair.

### ***SMAD3 experiments***

For SMAD3 compounds, given a limit of 10 compounds to study, we chose the top five positive matches and the top two negative matches (which were somewhat cytotoxic based on cell count in the Cell Painting assay), along with three additional negative matches (among the top 15) which were less cytotoxic. One was unavailable.

A549 lung carcinoma cells were transfected with the luciferase reporter plasmids 4xSBE-Luc to measure TGF- $\beta$ /Smad3-activated transcription<sup>53</sup> and pRL-TK (low expressing, constitutively active Renilla luciferase under the HSV-thymidine kinase promoter) (Promega cat# E224A) to normalize for the 4xSBE Firefly luciferase values. The transfected cell lysates were processed for luciferase assays as described<sup>56</sup> and per manufacturer’s protocol (Promega). In brief, the cells were seeded in 24-well plates at 80% confluency and, after adhering, the media was changed to growth or starvation media (RPMI-1640 with 10% or 2% FBS respectively) for 6 hours. The cells were then transfected with 200 ng 4xSBE-Luc and 100ng RI-Tk-Luc reporter plasmids per well using Lipofectamine 2000 per manufacturer recommendations (Thermo Fisher cat# 11668019). 12 hours after transfection cells were treated for 24 hours with 5 ng/ml TGF- $\beta$ 1 or 5  $\mu$ M SB431542 to inhibit TGF- $\beta$ -induced Smad activation, and either of 9 compounds at 10 $\mu$ M in triplicate. All cells were harvested with 200  $\mu$ l of passive lysis buffer (Promega). Luciferase assays were performed using a Dual-Luciferase assay kit (Promega), and luciferase activities were quantified with a SpectraMax M5 plate luminometer (Molecular Devices) and normalized to the internal Renilla luciferase control and DMSO control.

### ***Ras experiments***

Isogenic RAS-less mouse embryonic fibroblast cell lines driven by human KRAS4b G12D, HRAS WT, or BRAF V600E alleles were plated in 384-well plates and dosed with compound or DMSO 18 hours later using an Echo acoustic liquid handler in a 10 point, 2-fold dilution in 0.2% DMSO, with 10 $\mu$ M as the top concentration. After 72 hours, Promega CellTiter-Glo<sup>®</sup> reagent was added, and the signal was read using Envision software.

Values were normalized using day zero and DMSO control readings. Hits were determined by a one log difference in IC<sub>50</sub> values between BRAF V600E and RAS-driven cell line responses.

### ***Casein-kinase 1 alpha experiments***

CSNK1A1 enzymatic assays were performed by mobility shift assay using the Labchip EZ Reader II (Perkin Elmer). GST-tagged human CSNK1A1 (Carna Biosciences) protein was incubated with ATP, substrate, and assay buffer (20 mM Hepes - pH 7.5, 5 mM MgCl<sub>2</sub>, and 0.01% Triton X-100). The assay reaction was initiated with 5 μM ATP, 2 mM DTT, and 1 μM Profiler Pro FL-Peptide 16 substrate (Perkin Elmer). Curve fitting and determination of AC<sub>50</sub> values for phosphorylation inhibition were performed using Genedata.

### ***GSK3B experiments***

The compounds with a Cell Painting profile matching or opposing GSK3 overexpression were tested against GSK3α and GSK3β as previously reported<sup>54</sup>. Purified GSK3β or GSK3α was incubated with tested compounds in the presence of 4.3 μM of ATP (at or just below K<sub>m</sub> to study competitive inhibitors) and 1.5 μM peptide substrate (Peptide 15, Caliper) for 60 minutes at room temperature in 384-well plates (Seahorse Bioscience) in assay buffer that contained 100 mM HEPES (pH 7.5), 10 mM MgCl<sub>2</sub>, 2.5 mM DTT, 0.004% Tween-20, and 0.003% Brij-35. Reactions were terminated with the addition of 10 mM ethylenediaminetetraacetic acid (EDTA). Substrate and product were separated electrophoretically, and fluorescence intensity of the substrate and product was determined by Labchip EZ Reader II (Perkin Elmer). The kinase activity was measured as percent conversion to product. The reactions were performed in duplicate for each sample. The positive control, CHIR99021, was included in each plate and used to scale the data in conjunction with "in-plate" DMSO controls. The results were analyzed by Genedata Assay Analyzer. The percent inhibition was plotted against the compound concentration, and the IC<sub>50</sub> value was determined from the logistic dose-response curve fitting. Values are the average of at least three experiments. Compounds were tested using a 12-point dose curve with 3-fold serial dilution starting from 33 μM. The two most active compounds were resynthesized for validation and tested along with closely related analogs (Supplemental Methods).

### ***p38 experiments***

Cell Painting profiles for two wild-type variants of p38α (MAPK14) were averaged to create a p38α Cell Painting profile. 20 compounds whose Cell Painting profile correlated positively or negatively to that of p38α overexpression were selected; we also chose 14 "non-correlated" compounds (i.e. absolute value of correlation <0.2) as negative/neutral controls. The compounds were tested for their influence on p38 activity using the RPE1-p38 kinase translocation reporter (KTR) line that was previously generated<sup>24</sup>. This cell line has been tested and confirmed to be negative for mycoplasma contamination, but not authenticated. p38 activity is measured by phosphorylation of its substrate, MEF2C, which is preferentially phosphorylated by p38α, while p38β and p38δ contribute less<sup>55</sup>. RPE1-p38KTR cells were cultured in DMEM/F12 medium supplemented with 10% Fetal Bovine Serum at 37C in a humidified atmosphere with 5% CO<sub>2</sub>. 1000 cells were plated per well in 96-well plates and treated with 1μM and 10μM of each compound (n=4 well per concentration per compound, no replicates) for 48 hours. Only the middle 60 wells were used to prevent potential confounds from the edge effect. Cells were then fixed in 4% paraformaldehyde for 10min, followed by permeabilization in cold methanol at -20C for 5min. Cells were stained with 0.4 μg/mL Alexa Fluor 647 carboxylic acid, succinimidyl ester for 2hr at RT, followed by 1μg/mL DAPI for 10min at RT to facilitate the segmentation of individual cells.

p38 activity in single cells was calculated using the ratio of the median intensity of the p38-KTR in a 5-pixel-wide cytoplasmic ring around the nucleus to the median intensity of the p38-KTR in the nucleus. p38

activity measurements were normalized to DMSO within the same plate and column. The Student's t-test or Kolomogorov-Smirnov (KS) test was used to assess the significance of changes in the single cell distributions of p38 activity for each compound relative to control; we note that even for the positive control known inhibitor the effect sizes are small. When reporting hits from the assay, KS test and t-test p-values were adjusted to control the false discovery rate using the Benjamini-Hochberg method, using the `p.adjust(method="BH")` method in R.

### ***PPARGC1A (PGC-1 $\alpha$ ) experiments***

*Reporter assays:* To measure PGC-1 $\alpha$  activity related to PPARG, RT112/84 cells were obtained from the Cancer Cell Line Encyclopedia (Broad Institute, Cambridge, MA), which obtained them from the original source and performed cell line authentication. The cell line was engineered with the NanoLuc gene cloned into the 3' UTR of the FABP4 (previously described<sup>31</sup>) followed by stable expression of nuclear GFP (pTagGFP2-H2B, Evrogen) and tested negative for mycoplasma (MycoAlert, Lonza). Cells were plated in 384-well plates at ~10,000 cells/well and dosed with indicated compounds in the absence or presence of EC50 of PPARG agonist, rosiglitazone, using an HP D300 digital dispenser. The following day nuclei were counted for normalization (IncuCyte S3, Essen Bioscience) and the reporter activity was evaluated using the NanoGlo Luciferase Assay System (Promega). Normalized data is reported as NanoGlo arbitrary light units divided by cell number. PPARG agonist, rosiglitazone, and inhibitor, T0070907, were obtained from Tocris and included as controls.

To measure effects on PGC1 $\alpha$ /ERR $\alpha$ , HEK293T cells purchased from ATCC were co-transfected with Gal4-ERR $\alpha$ , with and without PGC1 $\alpha$  (pCDNA3.1-Flag-HA-PGC-1 $\alpha$ <sup>56</sup>), kind gifts from Pere Puigserver, in combination with the Gal4 UAS reporter construct, pGL4.35 [luc2P/9XGAL4UAS/Hygro] (Promega) modified by subcloning the HSV-TK promoter into the unique HindIII site that is downstream of the 9xGal4 UAS sites, in addition to a Renilla luciferase expression vector pRL (Promega) for normalization. Cells were dosed with compounds and 24 hours later, plates were analyzed using Dual-Glo Luciferase Assay System (Promega). Normalized light units are reported as Firefly luciferase divided by Renilla luciferase. ERR $\alpha$  modulators XCT790, Daidzein, and Biochanin A (Cayman Chemical) were included as controls. 293T cells were not authenticated nor tested for mycoplasma.

*High content mitochondrial motility screen:* We used our previously published assay to assess mitochondrial motility<sup>34</sup>. Briefly, we plated E18 rat cortical neurons in the middle 60 wells of 96 well plates (Greiner) – 40,000 cells per well in 150  $\mu$ l enriched Neurobasal media. Neurons were transfected with mito-DsRed at DIV7 using Lipofectamine2000 (Life Technologies). Plating and transfection were all done using an Integra VIAFLO 96/384 automated liquid handler. At DIV9, test compounds were added into wells to achieve a final concentration of 10  $\mu$ M each (4 wells per compound), as well at 10  $\mu$ M calcimycin for neg. control, and DMSO only for mock treatment. Following a 1-2 hour incubation, plates were imaged on a ArrayScan XTI (Thermo Fisher). Mitochondrial motility data was extrapolated from imaging data using a MATLAB and CellProfiler based computational pipeline. Compounds A01-A12 were tested on one plate; B01-B11 were tested separately on another plate on the same day. The experiment was repeated twice in different weeks. In the second week, TMRE was added to all wells after imaging was completed (20min, then 2 washes) and imaged to measure mitochondrial membrane potential in order to determine mitochondrial and cell health.

### ***YAP1-related compounds***

For the initial experiments, quality control of the compounds revealed that purity was 88% for A15 (BRD-K34692511-001-01-9), 81% for A05 (BRD-K28862419-001-01-9), and > 99% for E07

(BRD-K43796186-001-01-1). For subsequent experiments in the Eisinger lab, BRD-K43796186 (NB4A) was ordered from MuseChem (cat. #M189943) and for the Kiessling lab, from Ambinter (Cat # Amb2554311).

### ***YAP1 cell culture and treatments***

Eisinger lab: Murine KP230 cells, a Yap1-dependent cancer cell line, were derived from a tumor from the KP mouse model (*Kras*<sup>G12/D</sup>; *Trp53*<sup>fl/fl</sup>), as described in<sup>43</sup>. STS-109 UPS cells were derived from a human UPS tumor and validated by Rebecca Gladdy, MD (Sinai Health System, Toronto, Ontario, Canada). TC32 cells were a gift from Patrick Grohar, MD, PhD (Children's Hospital of Philadelphia). HT-1080, HCT-116, and HEK293T cells were purchased from ATCC. KP230, HT-1080, and HEK-293T cells were grown in DMEM with 10% FBS, 1% L-glutamine, and 1% penicillin/streptomycin (P/S). STS-109 cells were cultured in DMEM with 20% FBS, 1% L-glutamine, and 1% P/S. TC32 cells were grown in RPMI with 10% FBS, 1% L-glutamine, and 1% P/S. HCT-116 cells were cultured in McCoy's 5A medium with 10% FBS and 1% P/S. All cells were confirmed to be negative for mycoplasma contamination and were maintained in an incubator at 37C with 5% CO<sub>2</sub>. For experimental purposes, cells were cultured for up to 20 passages before being discarded, and were grown to approximately 50% confluence to circumvent the effects of high cell density on Yap1 expression and activity. All cell lines in the Eisinger laboratory were treated with 10 μM of each inhibitor or an equivalent volume of DMSO every 24 hours for 3 days, except for STS-109 cells, which were treated daily for 8 days.

Kiessling lab: H9 hPSCs (WiCell) were maintained on vitronectin (Thermo Fisher)-coated plates in Essential 8 (E8) medium. The cells were routinely passaged using 0.5mM EDTA and treated with 5μM Y-27632 dihydrochloride (Tocris) on the first day. For testing the effects of the small molecules, H9 hPSCs were seeded at 50K cells/cm<sup>2</sup> on vitronectin-coated plates in E8 medium supplemented with 5μM Y-27632 dihydrochloride (day 0). On day 1, the medium was switched to E8 medium. On day 2, the medium was switched to E8 medium supplemented with the small molecules. Following overnight incubation, the cells were collected for subsequent analysis on day 3. The cells were regularly checked for Mycoplasma contaminations (Sigma Aldrich - Lookout Mycoplasma PCR Detection Kit) but were not authenticated.

Boerckel lab: Murine periosteal cells were isolated from a transgenic mouse model (CMV-Cre;R26R-rtTA<sup>fl</sup>; tetO-YAP<sup>S127A</sup>; C57Bl/6 strain/background) in which YAP1 can be activated in a doxycycline inducible manner (Camargo 2011). This mouse model expresses a mutant form of YAP1 (YAP<sup>S127A</sup>) that escapes degradation. Cells were isolated from 3 female mice (age 15 weeks) from a 4-day old femoral fracture callus. Cells were cultured in a-MEM with 15% Fetal Bovine serum (S11550, R&D Systems), 1% GlutaMAX-I (Gibco, 35050-061) and 1% Penicillin/Streptomycin (Gibco, 15140-122).

### ***YAP1-related lentiviral production***

Knockdown of *YAP1* in HCT-116 cells was performed with shRNAs (TRC clone IDs: TRCN0000107266 and TRCN0000107267); a scrambled shRNA was used as a negative control. shRNA plasmids (Dharmacon) were packaged using the third-generation lentiviral vector system (pVSV-G, pMDLG, and pRSV-REV; Addgene) and expressed in HEK-293T cells using Fugene 6 transfection reagent (Promega). Virus-containing supernatants were collected 24 and 48 hours after transfection and concentrated 40-fold by centrifugation with polyethylene glycol 8000.

### ***YAP1-related proliferation assays***

NB4A treatment: Cells were treated with 10  $\mu\text{M}$  of each inhibitor or an equivalent volume of DMSO every 24 hours for 3-8 days, and counted with a hemocytometer with trypan blue exclusion daily (KP230, HT-1080, TC32, HCT-116), or every 2 days (STS-109).

shRNA-mediated *YAP1* knockdown: HCT-116 cells were infected with *YAP1* shRNA-encoding lentiviruses in the presence of 8  $\mu\text{g}/\text{mL}$  polybrene (Sigma). Antibiotic selection (3  $\mu\text{g}/\text{mL}$  puromycin) was performed after 48 hours, after which cells were cultured for an additional 48 hours. Cells were then trypsinized, seeded under puromycin-selection conditions, and counted with a hemocytometer with trypan blue exclusion on days 7, 8, and 9 post-infection.

### ***YAP1-related qRT-PCR***

For the Eisinger lab, total RNA from cultured cells was isolated with the QIAGEN RNeasy mini kit, and cDNA was synthesized with the High-Capacity RNA-to-cDNA kit (Life Technologies). qRT-PCR analysis was performed with TaqMan “best coverage” probes on a ViiA7 instrument. Hypoxanthine phosphoribosyltransferase (*HPRT*) and succinate dehydrogenase subunit A (*SDHA*) were used as endogenous controls. Relative expression was calculated using the ddCt method.

For the Kiessling lab, the RNA was extracted using TRIzol (Life Technologies) and Direct-zol™ RNA MiniPrep kit (Zymo Research) as per manufacturer instructions. The RNA was reverse transcribed using iScript cDNA synthesis kit (Bio-Rad). The qPCR was performed on CFX Connect (Bio-Rad) using iTaq Universal SYBR Green Supermix (Bio-Rad). GAPDH was used as a reference gene for normalization. The relative gene expression levels were determined using the ddCt method. The primer sequences used are listed in Supplementary Table S9.

For the Boerckel lab, to induce *YAP*<sup>S127A</sup>, 1  $\mu\text{M}$  doxycycline was added to the cell culture medium for 48 hours. This was used as a positive control to compare *YAP1* mRNA expression. Cells were also treated with BRD-K34692511-001-01-9 at 5  $\mu\text{M}$ . mRNA was isolated from cells (n=3/group/time point) at 1, 4 or 48 hours after treatment using Qiagen RNeasy Mini kit (Qiagen, 74106). cDNA was prepared as per the manufacturer’s protocol using the High-Capacity Reverse Transcription kit (ThermoFisher scientific, 4368814). qPCR analysis was performed using the QuantStudio 6 Pro Real-Time PCR System.

### ***YAP1-related reporter assay***

Varelas lab: HEK293T cells purchased from ATCC were co-transfected using Lipofectamine 3000 (Thermo Fisher) with a TEAD luciferase reporter construct, 8xGTIIIC-luciferase (gift from Stefano Piccolo, Addgene plasmid # 34615), a plasmid expressing Renilla Luciferase from a CMV promoter as a transfection control, along with a plasmid expressing 3xFlag-tagged wild-type *YAP1* from a CMV promoter (pCMV5 backbone). Following transfection the cells were immediately treated with 0.2% DMSO, 10  $\mu\text{M}$  NB4A, BRD-K34692511 or BRD-K28862419 and then lysed 48 hours later. Lysates were examined using the Dual-Luciferase Reporter Assay System (Promega) according to the manufacturer’s protocol and measured using a SpectraMax iD3 plate reader (Molecular Devices). Firefly Luciferase activity from the TEAD reporter was normalized to Renilla Luciferase activity and then plotted as relative values. Mycoplasma tests are routinely performed, but cells were not recently authenticated.

### ***YAP1-related RNA-sequencing and data analysis***

Total RNA from cultured cells was isolated with the QIAGEN RNeasy Mini Kit with on-column DNase digestion. RNA quality checks were performed with an Agilent 2100 Bioanalyzer (Eukaryotic Total RNA Nano kit). Library preparation (500 ng input RNA) was performed with the NEBNext Poly(A) mRNA Magnetic Isolation Module (#E7490) with SPRIselect Beads (Beckman Coulter), the NEBNext Ultra II Single-End RNA Library Prep kit (#7775S), and the NEBNext Multiplex Oligos for Illumina (Index Primers Set 1) according to the manufacturer's instructions. Library size was confirmed with an Agilent 2100 Bioanalyzer (DNA1000 chip). Pooled libraries were diluted to 1.8 pM (concentrations checked with the Qubit Fluorometer high-sensitivity assay, Thermo Fisher), and sequenced on an Illumina NexSeq 500 instrument with the NexSeq 500 75-cycle high-output kit.

For data analysis, FASTQ files were generated with the *bcl2fastq* command line program (Illumina). Transcript alignment was performed with Salmon<sup>57</sup>. Differential expression analysis (NB4A- vs. DMSO-treated cells) was performed with the DESeq2 R package. DESeq2 "stat" values for each gene were used as inputs to pre-ranked GSEA, where enrichment was tested against the Hallmark gene sets from the Molecular Signatures Database (MSigDB). Access to sequencing data is discussed in the data availability section.

### ***YAP1-related Western blotting***

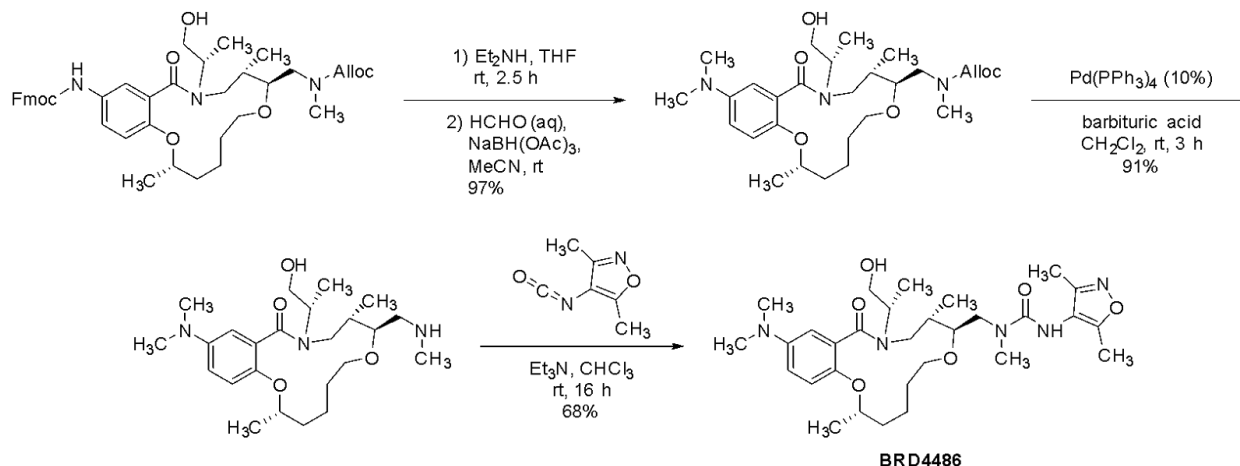
For the Kiessling lab, the cells were lysed in RIPA buffer (Pierce) supplemented with Halt Protease inhibitor cocktail and Halt Phosphatase inhibitor cocktail (Thermo Fisher). The Eisinger lab lysed cells in hot Tris-SDS buffer (pH 7.6) and boiled for 5 minutes at 95°C. The protein concentration of each sample was quantified using the Pierce BCA protein assay (Thermo Fisher). The proteins were resolved by SDS-PAGE and transferred to PVDF membranes using the Trans-Blot Turbo Transfer system (Bio-Rad). The membranes were blocked in 5% non-fat milk in TBS-T for up to 1 hour at room temperature and incubated with primary antibodies in 5% bovine serum albumin in TBS-T overnight at 4°C. Then, the membranes were incubated with HRP-conjugated anti-rabbit IgG secondary antibodies at 1:10000 (Kiessling lab; Jackson ImmunoResearch Laboratories, #111-035-003) or 1:2500 (Eisinger lab; Cell Signaling Technology [CST] #7074) for 1 hour at RT and developed in the ChemiDoc MP Imaging system (Kiessling lab) or on autoradiography film (Eisinger lab) using ECL Prime reagent (Amersham). The band intensities in immunoblots were quantified with Image Lab software. The primary antibodies and dilutions used are: anti-YAP1 (CST 4912S and CST 14074 [clone D8H1X]) at 1:1000, anti-phospho-YAP1-S127 (CST 4911S) at 1:1000, and anti-GAPDH (CST 5174 and CST 2118 [clone 14C10]) at 1:15000 and 1:1000, respectively. Primary antibodies were validated commercially in cells both wild-type and deficient (e.g., knockout) for the gene/protein of interest. YAP1-related immunofluorescence and image analysis

For the Eisinger lab, cells grown on poly-L-lysine-coated chamber slides were fixed in 4% PFA (15 minutes at room temperature), permeabilized with 0.5% Triton-X100/PBS (15 minutes at room temperature), and blocked with 5% goat serum (Vector Laboratories S-1000; 1 hour at room temperature). Cells were then incubated with anti-Yap1 primary antibodies (CST #14074 [clone D8H1X]; 1:1000) diluted in blocking buffer overnight at 4°C. Subsequently, cells were incubated with Alexa Fluor 488-conjugated secondary antibodies (4 ug/mL in blocking buffer; Thermo Fisher Scientific #A-11008) for 1 hour at room temperature. Coverslip mounting was performed with ProLong Gold Antifade reagent with DAPI. Images (5 fields per condition for each of 3 independent experiments) were acquired with a Nikon Eclipse Ni microscope and Nikon NES Elements software. Image analysis was performed with Fiji as follows: For nuclear staining intensity, watershed analysis of DAPI channel images (8-bit) was performed to "separate" nuclei that appeared to be touching. Nuclei were then converted to regions of interest (ROIs) that were "applied" to the corresponding GFP channel image (8-bit format). Analysis of staining intensity in these nuclear ROIs was then performed, excluding objects smaller than 100 pixels<sup>2</sup> (integrated density normalized to number of nuclei). A similar process was followed to

determine whole-cell staining intensity: using 8-bit GFP channel images, cells were distinguished from background via thresholding, and converted to ROIs that were applied back to the 8-bit GFP channel images. Analysis of staining intensity (integrated density normalized to number of nuclei) was then performed in these ROIs, excluding objects smaller than 500 pixels<sup>2</sup>. The ratio of nuclear to total Yap1 expression was determined after subtracting out background GFP signal from no-primary antibody controls.

For the Kiessling lab, the cells were fixed with 4% formaldehyde for 15 mins at room temperature. The cells were permeabilized and blocked with PBS containing 2% BSA and 0.1% Triton-X100. The cells were incubated with a primary antibody against YAP1 (Santa Cruz Biotechnology, sc-101199) at 1:200 dilution in a blocking buffer overnight at 4°C. Then, the cells were incubated with a goat anti-mouse Alexa Fluor 488 conjugated secondary antibody (Thermo Fisher, #A11001) at 1:1000 dilution for 1 hour at room temperature. The nuclei were counterstained with DAPI dilactate (Molecular Probes). Images were collected with Olympus FV1200 microscope and analyzed with CellProfiler. Briefly, nuclei and cell bodies were segmented using DAPI and YAP channels respectively. The cell cytoplasm was determined as the region outside nuclei but within the cell bodies. Then, the ratio of mean intensity of YAP in the nucleus to cytoplasm was calculated to determine YAP translocation.

### Chemical synthesis of BRD4486



We followed prior work<sup>58</sup>. To a solution of the Fmoc-protected intermediate (100 mg, 0.140 mmol, 1 eq) in tetrahydrofuran (1 mL) was added diethylamine (150 μL, 1.44 mmol, 10.3 eq). The mixture was stirred 2.5 h, and the solvent and excess amine were evaporated.

The residue was dissolved in acetonitrile (1 mL), then formaldehyde (37% aqueous, 100 μL, 1.32 mmol, 9.4 eq), catalytic acetic acid (1 drop), and sodium triacetoxyborohydride (100 mg, 0.472 mmol, 3.4 eq) were added. The mixture was stirred 1 h, then quenched with saturated aqueous NaHCO<sub>3</sub> and diluted with CH<sub>2</sub>Cl<sub>2</sub>. The layers were separated, and the aqueous layer was extracted with CH<sub>2</sub>Cl<sub>2</sub>. The combined organic layers were dried over MgSO<sub>4</sub>, filtered, and evaporated, and the residue was purified by flash column chromatography (0-10% MeOH/CH<sub>2</sub>Cl<sub>2</sub>) to provide the dimethylaniline (70.2 mg, 97% yield).

A yellow solution of the resulting Alloc-protected amine (68 mg, 0.131 mmol, 1 eq), 1,3-dimethyl-barbituric acid (200 mg, 1.28 mmol, 9.8 eq), and tetrakis(triphenylphosphine)palladium(0) (15 mg, 0.013 mmol, 0.1 eq) in dichloromethane (1 mL) was stirred at room temperature for 3 h. The reaction was quenched with 0.1 M HCl and stirred 15 min. The layers were separated, and the organic layer was extracted with 0.1 M HCl. The pH of the combined aqueous layers was adjusted to ~12 with 4 M NaOH, then extracted with CH<sub>2</sub>Cl<sub>2</sub>. The combined organic layers were dried over Na<sub>2</sub>CO<sub>3</sub>,

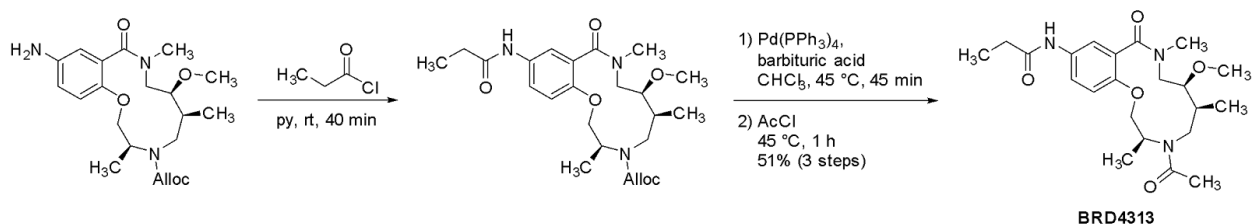


filtered, and evaporated to provide the crude free amine (52 mg, 91% yield), which was used directly in the urea formation.

To a solution of the crude secondary amine (52 mg, 0.119 mmol, 1 eq) and 3,5-dimethylisoxazol-4-yl isocyanate (20 mg, 0.145 mmol, 1.2 eq) in chloroform (1 mL) was added triethylamine (16.5  $\mu$ L, 0.119 mmol, 1 eq). The mixture was stirred at room temperature for 16 h, and the solvent was evaporated. The residue was purified by flash column chromatography (0-10% MeOH/ $\text{CH}_2\text{Cl}_2$ ) to provide **BRD4486** (46.2 mg, 68% yield) as a white solid.

MS: 574.5  $[\text{M}+\text{H}]^+$ ; 572.3  $[\text{M}-\text{H}]^-$

### Chemical synthesis of BRD4313



We followed prior work<sup>59</sup>. To the aniline intermediate (100 mg, 0.247 mmol, 1 eq) dissolved in pyridine (0.5 mL) was added propionyl chloride (45  $\mu$ L, 0.514 mmol, 2.1 eq). The resulting mixture was stirred at room temperature for 40 min.

Chloroform (0.5 mL) and 1,3-dimethylbarbituric acid (385 mg, 2.46 mmol, 10 eq) were added, and, after 5 min, tetrakis(triphenylphenylphosphine)palladium(0) (28 mg, 0.024 mmol, 0.1 eq) was added. The yellow-green solution was stirred at 45 °C for 45 min ( $\text{CO}_2$  evolution), then acetyl chloride (261  $\mu$ L, 3.69 mmol, 15 eq) was added. After stirring 1 h, the mixture was diluted with  $\text{CH}_2\text{Cl}_2$  and poured into 0.1 M HCl. The layers were separated, and the aqueous layer was extracted with  $\text{CH}_2\text{Cl}_2$ . The combined organic layers were washed with saturated aqueous  $\text{NaHCO}_3$ , dried over  $\text{MgSO}_4$ , filtered, and evaporated. The residue was purified by flash column chromatograph (2.5-10% MeOH/ $\text{CH}_2\text{Cl}_2$ ) to provide the product (82.4 mg) in 84% purity. The material was further purified by mass-directed prep-HPLC (0-100% MeCN/water + 0.1% TFA) to provide **BRD4313** (54.6 mg, 51% yield over 3 steps) as a tan solid.

MS: 420.8  $[\text{M}+\text{H}]^+$

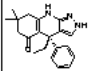
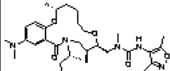
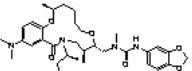
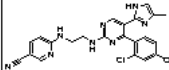
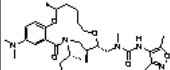
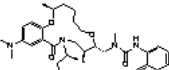
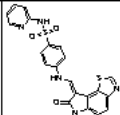
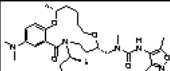
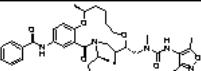
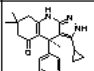
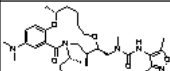
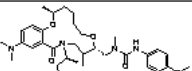
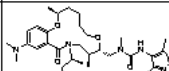
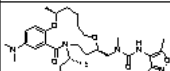
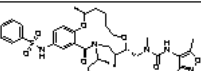
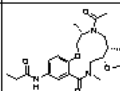
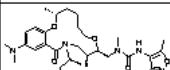
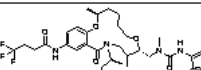
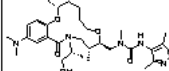
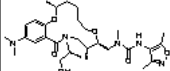
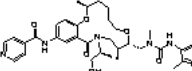
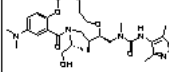
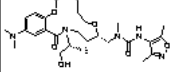
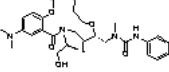
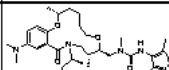
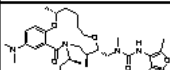
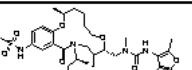
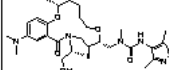
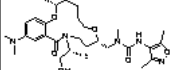
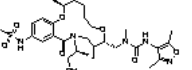
### Analog selection for GSK experiments

Compounds for (stereochemical) structure-activity relationship determination were selected from the Broad compound library in the following order until 24 analogs had been reached for each hit:

- 1) All available stereoisomers of the hit compound
- 2) Available regioisomers of the hit compound
- 3) Analogues with high structural similarity (Tanimoto  $\geq 0.75$ ) to the hit compound, selected for chemical diversity

Assay plates for each series (RCM/H2T) were prepared with 4 on-plate controls plus the hit compound from the opposing series. The controls included 3 dual GSK3 $\alpha/\beta$  inhibitors (CHIR-99021, GW8510, and BRD0320) and one GSK3 $\alpha$ -specific inhibitor (BRD0705). All compounds tested are shown below.

# BRD4486 (RCM) Series Assay Plate

Core ID	Structure	Note	Core ID	Structure	Note	Core ID	Structure	Note
BRD-K00760705		control	BRD-K94445007		RCM stereoisomer	BRD-K07274638		RCM analog
<b>CHIR99021</b> BRD-K16189898		control	BRD-K23628938		RCM stereoisomer	BRD-K18142082		RCM analog
<b>GW8510</b> BRD-K55000304		control	BRD-K36176998		RCM stereoisomer	BRD-K07891707		RCM analog
BRD-K87550320		control	BRD-K94445007		RCM stereoisomer	BRD-K26973634		RCM analog
BRD-K26994486		RCM hit	BRD-K10781609		RCM stereoisomer	BRD-K57195030		RCM analog
BRD-K91354313		H2T hit	BRD-K34254821		RCM stereoisomer	BRD-K71568523		RCM analog
BRD-K97242998		RCM stereoisomer	BRD-K65054381		RCM stereoisomer	BRD-K72681403		RCM analog
BRD-K56373119		RCM stereoisomer	BRD-K09376136		RCM stereoisomer	BRD-K61284358		RCM analog
BRD-K86938753		RCM stereoisomer	BRD-K12710356		RCM stereoisomer	BRD-K18599462		RCM analog
BRD-K59522787		RCM stereoisomer	BRD-K96280720		RCM stereoisomer	BRD-K55276005		RCM analog

## BRD4313 (H2T) Series Assay Plate

Core ID	Structure	Note	Core ID	Structure	Note	Core ID	Structure	Note
BRD-K00760705		control	BRD-K74022101		H2T stereoisomer	BRD-K74198088		H2T regio/stereoisomer
<b>CHIR99021</b> BRD-K16189898		control	BRD-K83538063		H2T stereoisomer	BRD-K06631334		H2T analog
<b>GW8510</b> BRD-K55000304		control	BRD-K97378175		H2T stereoisomer	BRD-K28720546		H2T analog
BRD-K87550320		control	BRD-K00411149		H2T regio/stereoisomer	BRD-K31377965		H2T analog
BRD-K91354313		H2T hit	BRD-K04403306		H2T regio/stereoisomer	BRD-K33863933		H2T analog
BRD-K26994486		RCM hit	BRD-K11844860		H2T regio/stereoisomer	BRD-K44217085		H2T analog
BRD-K12299093		H2T stereoisomer	BRD-K20077349		H2T regio/stereoisomer	BRD-K48114548		H2T analog
BRD-K42803695		H2T stereoisomer	BRD-K34274486		H2T regio/stereoisomer	BRD-K58769468		H2T analog
BRD-K53538949		H2T stereoisomer	BRD-K54036439		H2T regio/stereoisomer	BRD-K76966915		H2T analog
BRD-K61699306		H2T stereoisomer	BRD-K59865704		H2T regio/stereoisomer	BRD-K80986480		H2T analog

### Mobility shift microfluidics assay protocol

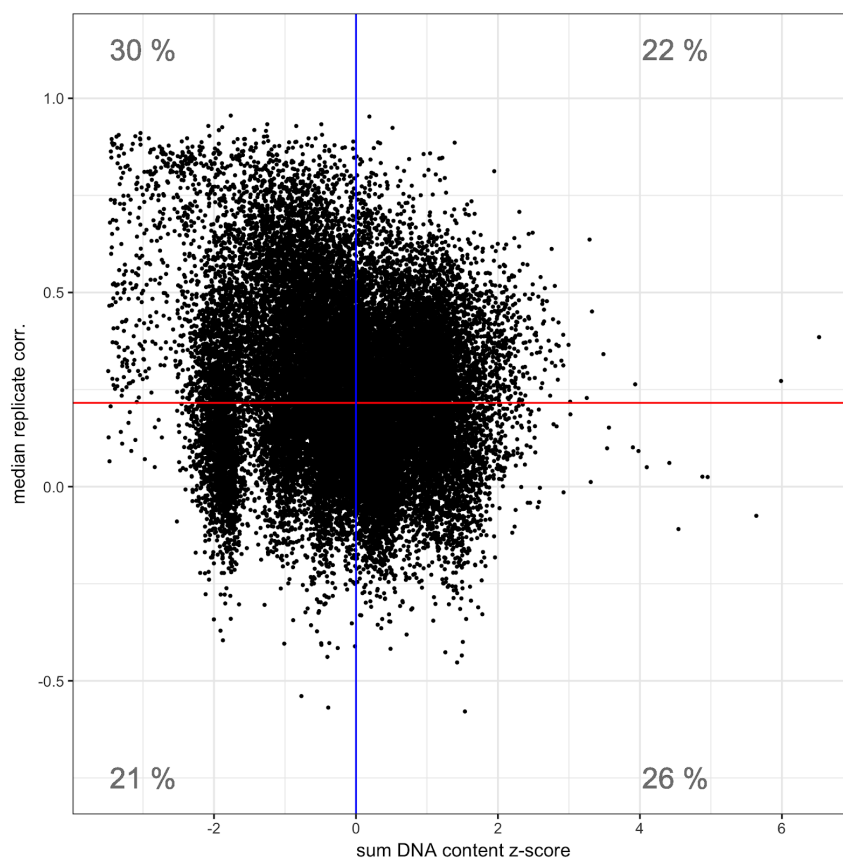
We followed previous protocol<sup>54</sup>. Purified GSK3 $\beta$  or GSK3 $\alpha$  was incubated with tested compounds in the presence of 4.3  $\mu$ M of ATP (at or just below  $K_m$  to study competitive inhibitors) and 1.5  $\mu$ M peptide substrate (Peptide 15, Caliper) for 60 minutes at room temperature in 384-well plates (Seahorse Bioscience) in assay buffer that contained 100 mM HEPES (pH 7.5), 10 mM MgCl<sub>2</sub>, 2.5 mM DTT, 0.004% Tween-20, and 0.003% Brij-35. Reactions were terminated by the addition of 10 mM ethylenediaminetetraacetic acid (EDTA). Substrate and product were separated electrophoretically, and fluorescence intensity of the substrate and product was determined by Labchip EZ Reader II (Caliper Life Sciences). The kinase activity was measured as percent conversion. The reactions were performed in duplicate for each sample. The positive control, CHIR99021, was included in each plate and used to scale the data in conjunction with in-plate DMSO controls. The results were analyzed by Genedata Assay Analyzer. The percent inhibition was plotted against the compound concentration, and the IC<sub>50</sub> value was determined from the logistic dose-response curve fitting. Values are the average of at least three experiments. Compounds were tested using a 12-point dose curve with 3-fold serial dilution starting from 33  $\mu$ M.

## Assay Results

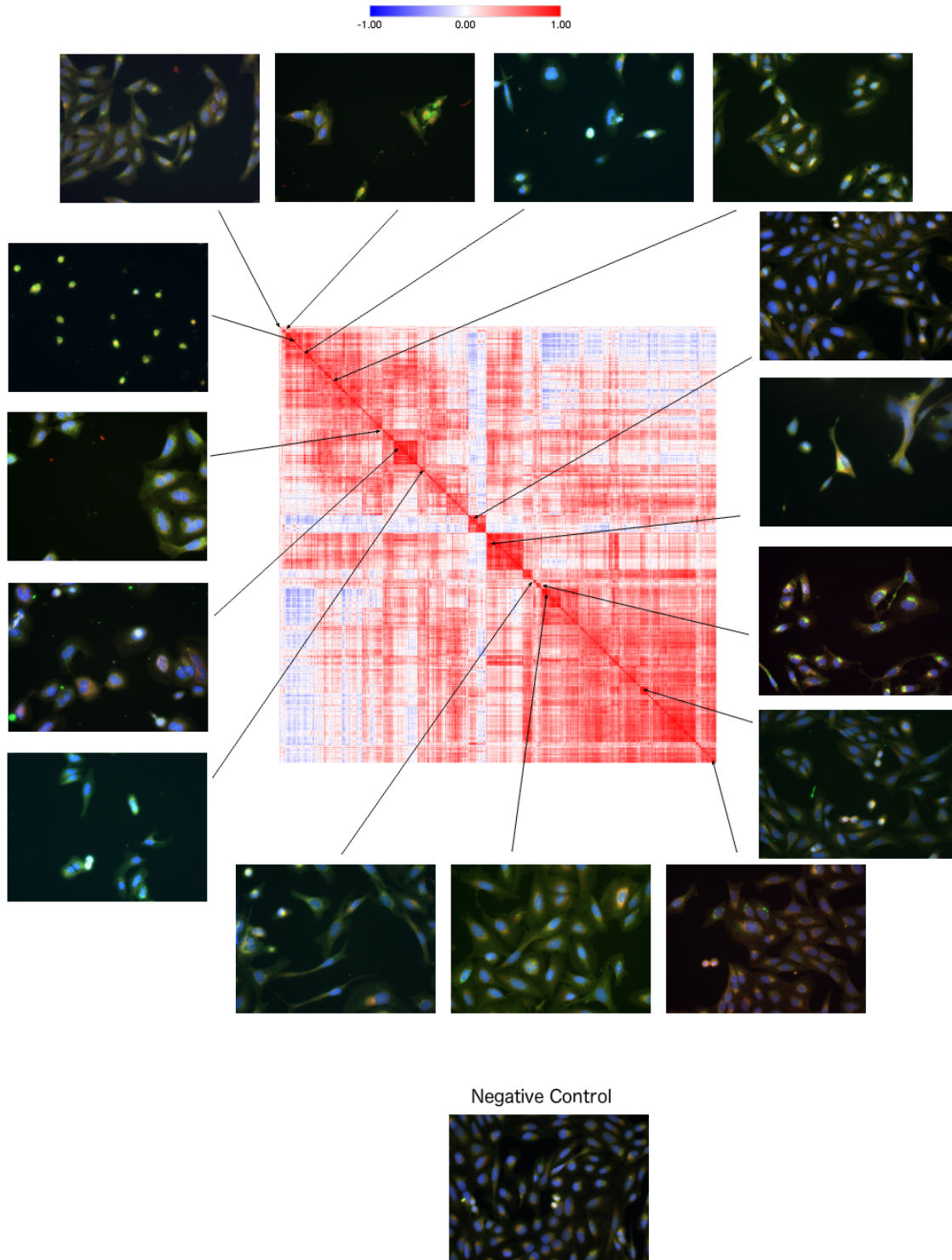
RCM		
Core ID	GSK3 $\alpha$ IC <sub>50</sub> $\mu$ M	GSK3 $\beta$ IC <sub>50</sub> $\mu$ M
BRD-K00760705	0.110	0.517
BRD-K16189898	0.00279	0.00254
BRD-K55000304	0.0198	0.00947
BRD-K87550320	0.0110	0.00530
BRD-K26994486	>33	>33
BRD-K91354313	>33	>33
BRD-K97242998	>33	>33
BRD-K56373119	>33	>33
BRD-K86938753	>33	>33
BRD-K59522787	>33	>33
BRD-K94445007	>33	>33
BRD-K23628938	>33	>33
BRD-K36176998	>33	>33
BRD-K94445007	>33	>33
BRD-K10781609	>33	>33
BRD-K34254821	>33	>33
BRD-K65054381	>33	>33
BRD-K09376136	>33	>33
BRD-K12710356	>33	>33
BRD-K96280720	>33	>33
BRD-K07274638	>33	>33
BRD-K18142082	>33	>33
BRD-K07891707	>33	>33
BRD-K26973634	>33	>33
BRD-K57195030	>33	>33
BRD-K71568523	>33	>33
BRD-K72681403	>33	>33
BRD-K61284358	>33	>33
BRD-K18599462	>33	>33
BRD-K55276005	>33	>33

H2T		
Core ID	GSK3 $\alpha$ IC <sub>50</sub> $\mu$ M	GSK3 $\beta$ IC <sub>50</sub> $\mu$ M
BRD-K00760705	0.121	0.583
BRD-K16189898	0.00538	0.00371
BRD-K55000304	0.0125	0.00693
BRD-K87550320	0.0195	0.00802
BRD-K91354313	>33	>33
BRD-K26994486	>33	>33
BRD-K12299093	>33	>33
BRD-K42803695	>33	>33
BRD-K53538949	>33	>33
BRD-K61699306	>33	>33
BRD-K74022101	>33	>33
BRD-K83538063	>33	>33
BRD-K97378175	>33	>33
BRD-K00411149	>33	>33
BRD-K04403306	>33	>33
BRD-K11844860	>33	>33
BRD-K20077349	>33	>33
BRD-K34274486	>33	>33
BRD-K54036439	>33	>33
BRD-K59865704	>33	>33
BRD-K74198088	>33	>33
BRD-K06631334	>33	>33
BRD-K28720546	>33	>33
BRD-K31377965	>33	>33
BRD-K33863933	>33	23.8
BRD-K44217085	>33	>33
BRD-K48114548	>33	>33
BRD-K58769468	>33	>33
BRD-K76966915	>33	>33
BRD-K80986480	>33	>33

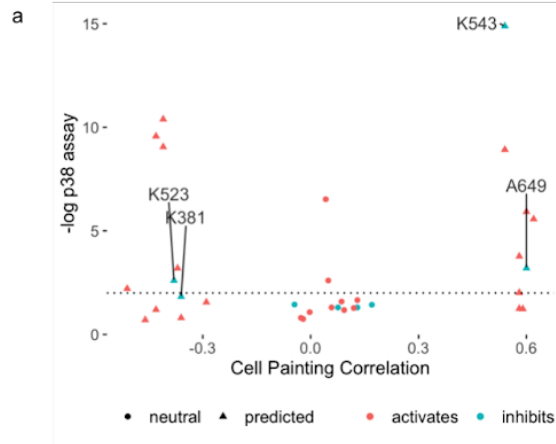
## Supplementary Figures:



**Supplementary Figure S1: Relationship between detectable Cell Painting profiles and cell proliferation rules out toxicity being a single, dominant phenotype.** The Y axis shows the replicate correlation, which is high for compounds that produce detectable morphological phenotypes in the Cell Painting assay. 52% of the compounds have a replicate correlation higher than the 95th percentile of non-replicate correlations (red line) and thus are considered to have a detectable phenotype. The X axis shows the z-score for the sum of DNA content, where higher values represent higher cell proliferation. Although the ratio of low-proliferation samples (left of blue line) with a detectable phenotype (30% vs. 21%) is higher than for high-proliferation samples (right of blue line) (22% vs. 26%), it is clear that impact on cell proliferation does not explain the majority of detectable morphological phenotypes. This fact is also supported by observing no significant negative correlation between proliferation and replicate correlation.



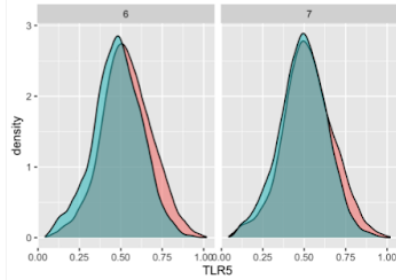
**Supplementary Figure S2: Compounds yielding a low cell count may be toxic or proliferation-impeding but they display many distinguishable phenotypes.** Low-cell-proliferation or potentially toxic compounds (with the z-score for the sum of DNA content less than -3) are clustered, and show many different types of toxic phenotype. Various tight clusters mean the assay is specific and has sufficient resolution to distinguish types of toxicity.



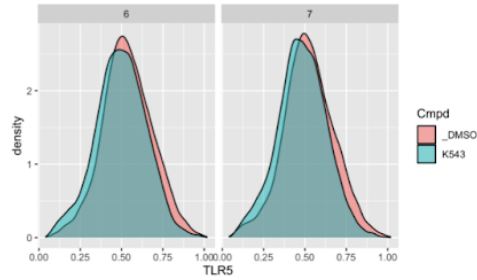
1  $\mu$ M

10  $\mu$ M

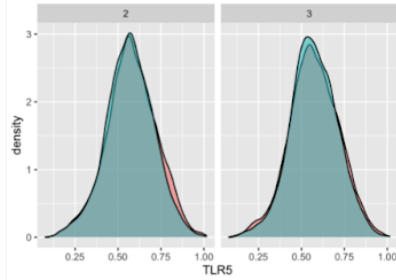
**b** cphit\_K543\_1  
ks\_stat = 0.11 ks\_pval = 1.1e-16 t\_stat = -17.9 t\_pval = 5.7e-27 cp\_cor = 0.54



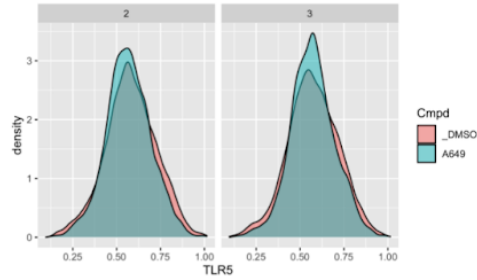
**c** cphit\_K543\_10  
ks\_stat = 0.10 ks\_pval = 5.7e-15 t\_stat = -15.6 t\_pval = 1.5e-20 cp\_cor = 0.54



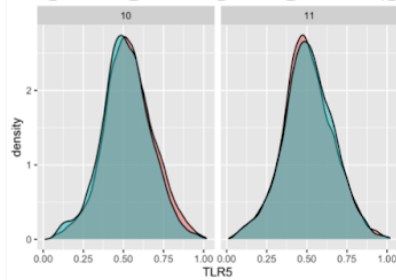
**d** cphit\_A649\_1  
ks\_stat = 0.06 ks\_pval = 0.00022 t\_stat = -2.5 t\_pval = 3.7e-05 cp\_cor = 0.60



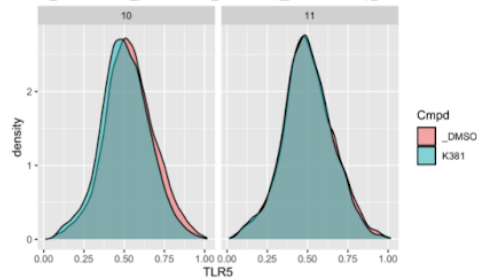
**e** cphit\_A649\_10  
ks\_stat = 0.06 ks\_pval = 0.00028 t\_stat = -2.6 t\_pval = 0.21 cp\_cor = 0.60



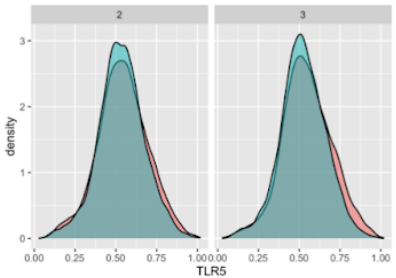
**f** cphit\_K381\_1  
ks\_stat = 0.05 ks\_pval = 0.0088 t\_stat = -2.5 t\_pval = 1.9e-05 cp\_cor = -0.36



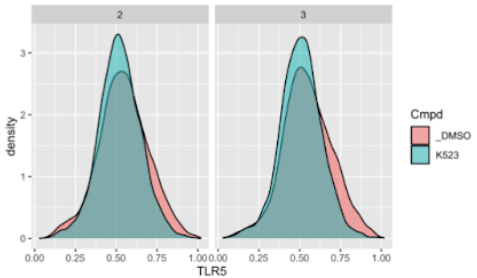
**g** cphit\_K381\_10  
ks\_stat = 0.05 ks\_pval = 0.025 t\_stat = -6.5 t\_pval = 0.041 cp\_cor = -0.36



**h** cphit\_K523\_1  
ks\_stat = 0.07 ks\_pval = 0.001 t\_stat = -6.0 t\_pval = 0.094 cp\_cor = -0.38



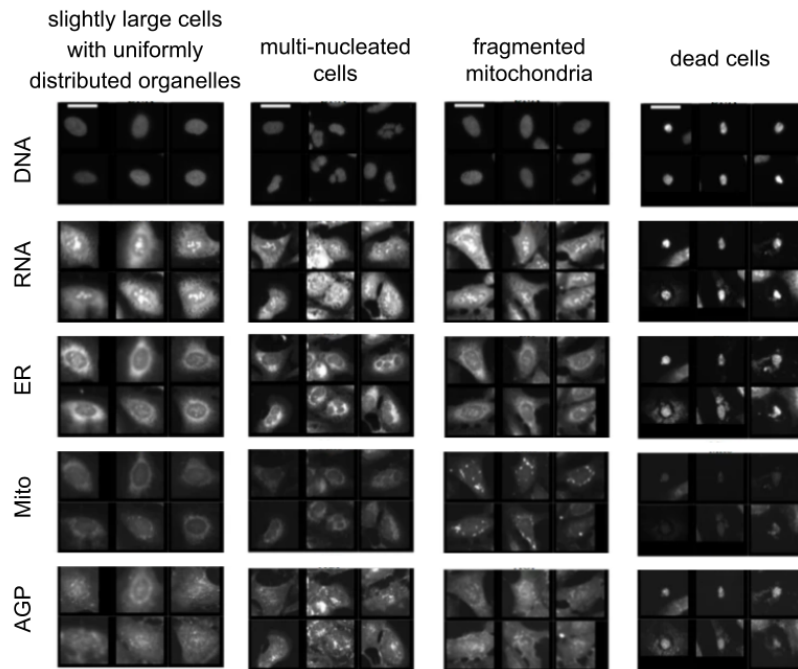
**i** cphit\_K523\_10  
ks\_stat = 0.11 ks\_pval = 3.7e-15 t\_stat = -10.5 t\_pval = 9.9e-12 cp\_cor = -0.38



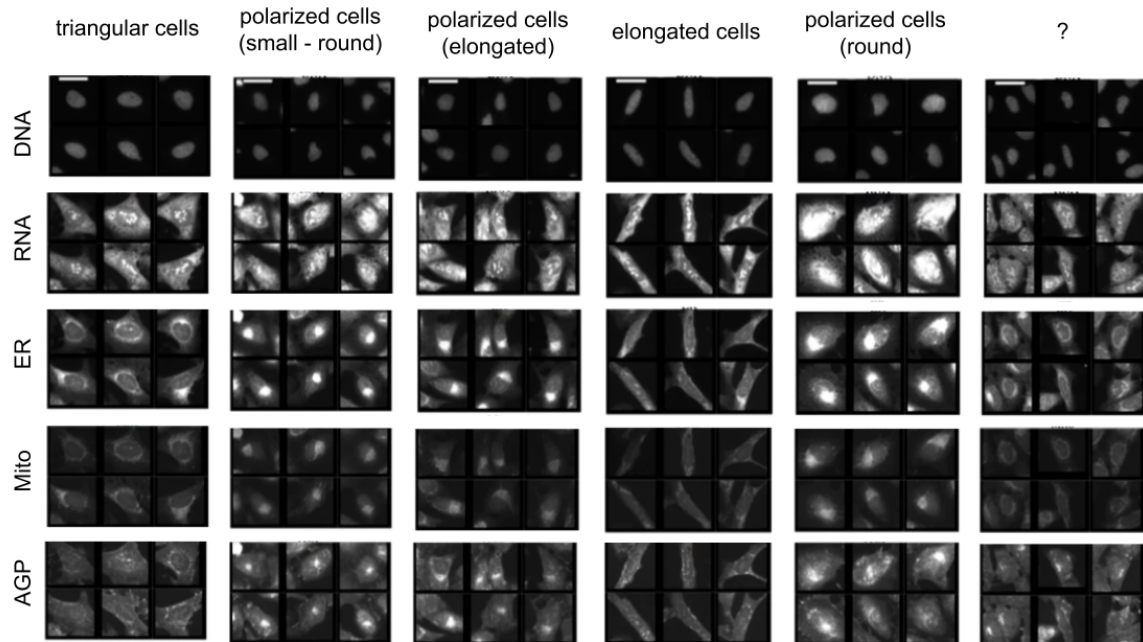
**Supplementary Figure S3: Predicted compounds impact p38 activity in a single-cell reporter assay.** a) The same experiment as shown in Figure 2 is shown here, except using a Kolmogorov-Smirnov (KS) analysis to detect differences in distribution instead of shifts in the mean. This raises an additional hit, K523. b-i) Single cell distribution plots show the shifts induced, at both 1 $\mu$ M and 10 $\mu$ M, by a known inhibitor of p38, SB202190 (b-c), by the two hits from the t-test in Figure 2 (d-g) and by the hit from the KS test (h-i). Note that the biological effect size here is relatively small, even for the known p38 inhibitor; this is typical for the assay.



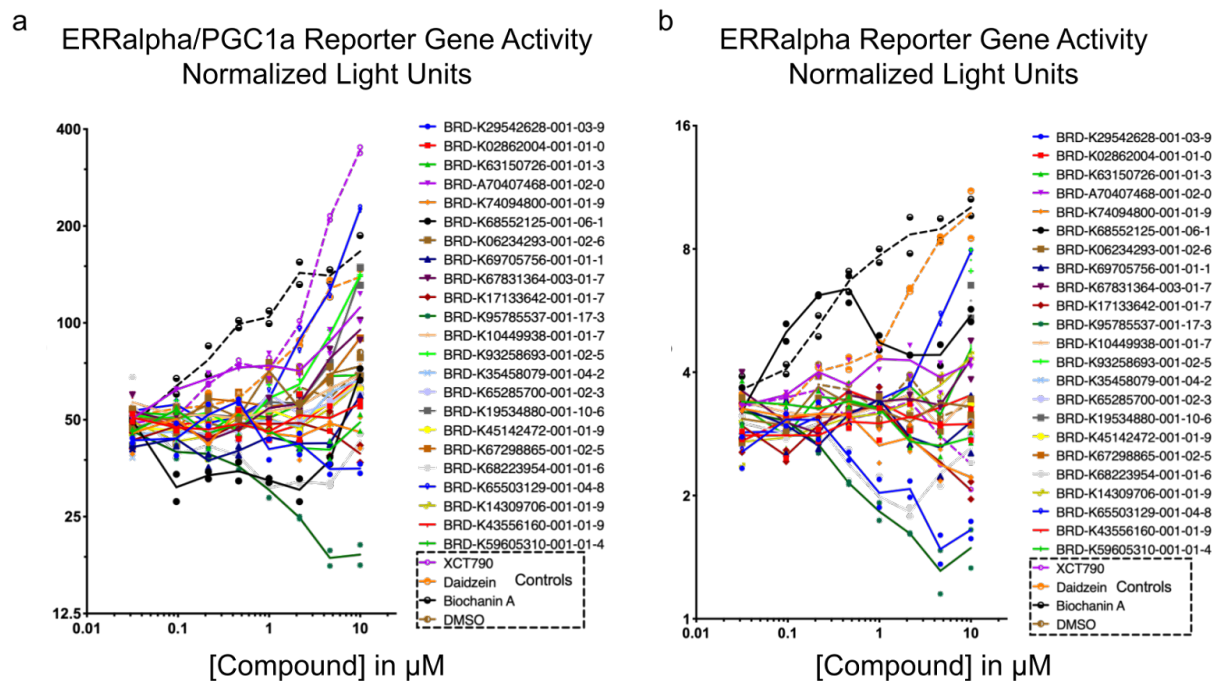
a Over-represented in the following subpopulations:



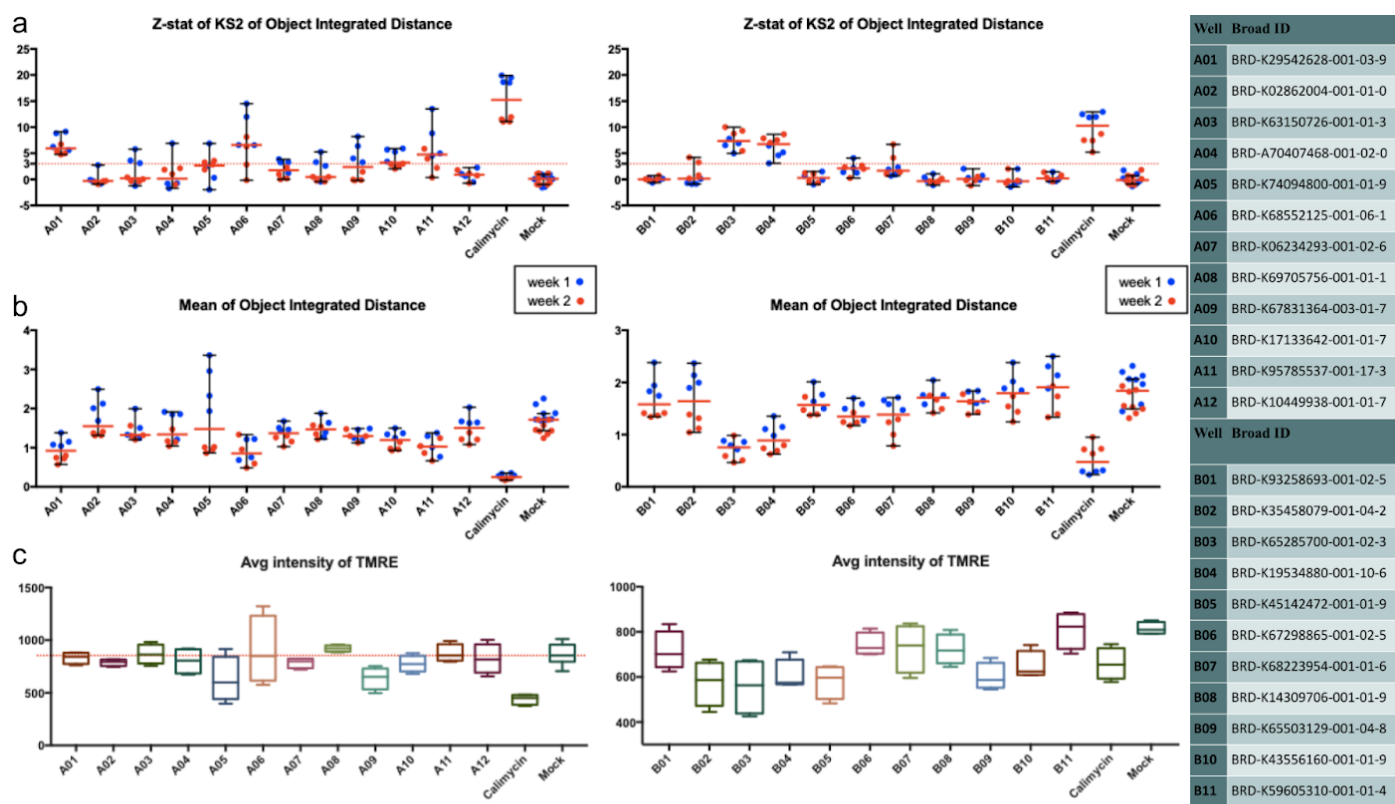
b Under-represented in the following subpopulations:



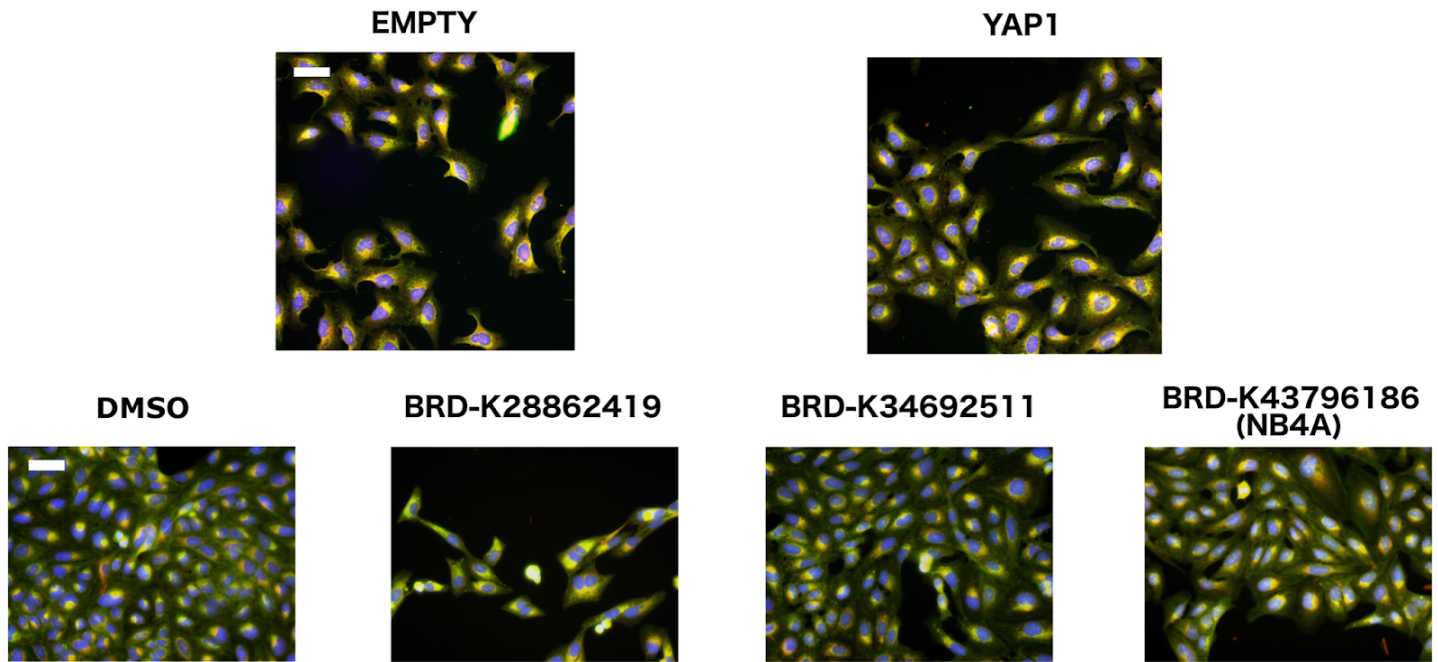
**Supplementary Figure S4: Certain subpopulations of cells are over- or under-represented when *PPARGC1A* is overexpressed.** Following the procedure described previously<sup>14</sup> we clustered cells based on their morphological profiles, then identified which subpopulations were (a) over- or (b) under-represented when *PPARGC1A* is overexpressed. Scale bars = 39.36  $\mu\text{m}$ .



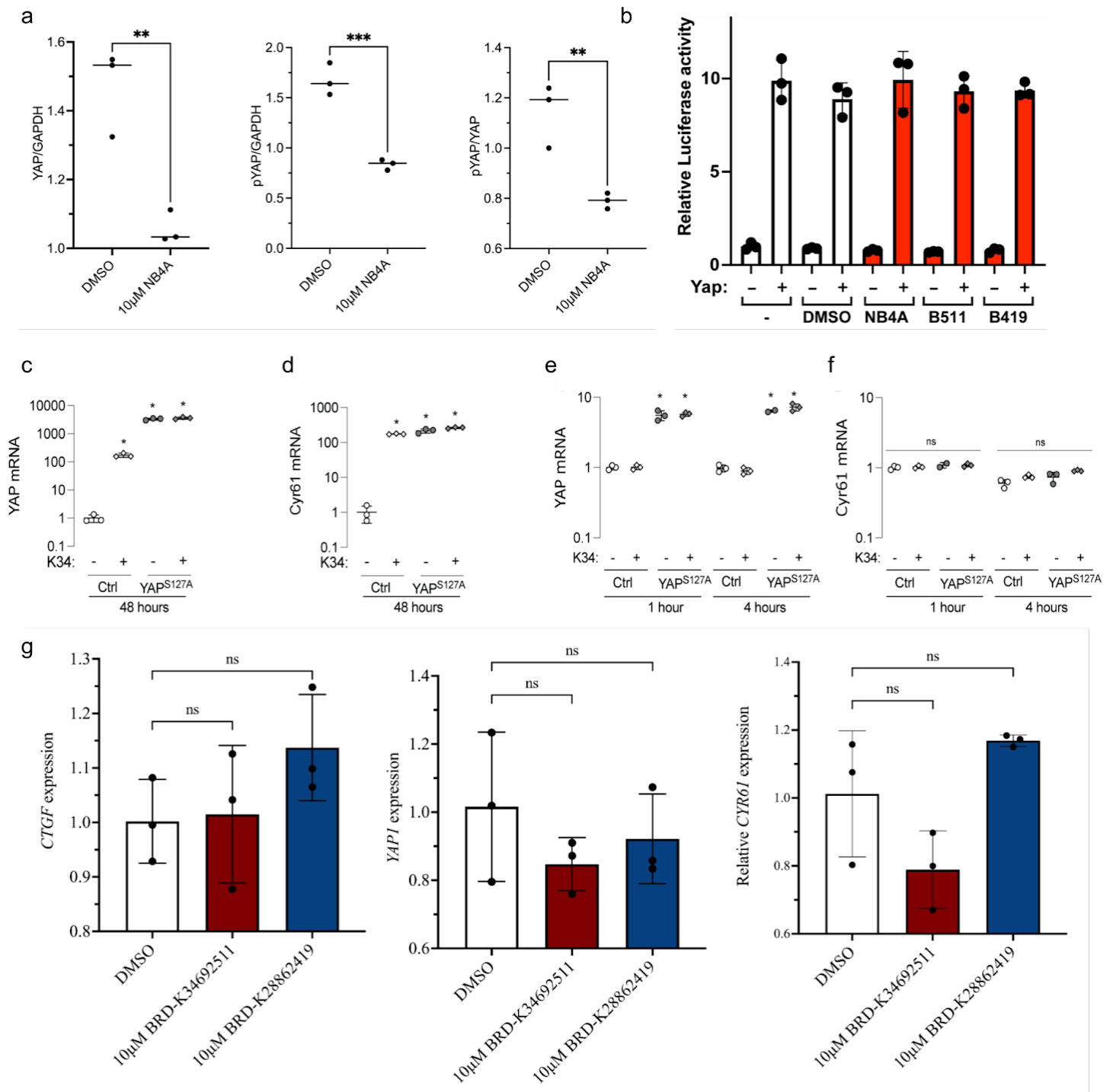
**Supplementary Figure S5: Compounds predicted to influence pathways containing PGC1 $\alpha$  impact an ERR $\alpha$  reporter assay in 293T cells.** In this reporter system, a mammalian one-hybrid fusion protein containing the Gal4 DNA binding domain and the ERR alpha ligand binding domain is co-expressed with the Firefly luciferase gene under control of the Gal4 Upstream Activating Sequence. Renilla luciferase was included for normalization. The assay was performed in the presence (a) or absence (b) of ectopically expressed PGC1 $\alpha$ ; their behavior being similar in these two conditions suggests, but does not prove, that the compounds do not directly target PGC1 $\alpha$  but instead modulate other targets in the relevant pathway, consistent with having been discovered by the morphological matching approach which assesses impact on the cell system rather than a particular desired target.



**Supplementary Figure S6: Predicted compounds impact a mitochondrial motility assay in rat cortical neurons.** (a) For most compounds, the integrated distance traveled for each motile mitochondrion (the length of travel, or the sum of all movements, including changes in direction) is comparable to the negative control (Mock), but a few (A01, A06, A10, A11, B03, and B04) consistently have a z-score  $>3$ , as does the positive control, Calcimycin, a calcium ionophore that arrests mitochondria<sup>60</sup>. Two separate experiments are plotted (week 1 in blue and week 2 in red), and the values are the Z-prime factor of the Kolmogorov-Smirnov (KS) statistic calculated for each compound. The red line indicates the median  $\pm$  95% confidence interval. (b) Mean values of the mitochondrial distance; these are the values that underlie the statistical analysis in (a). The red line indicates the median  $\pm$  95% confidence interval. (c) The average intensity of TMRE reflects the mitochondrial membrane potential, a measure of mitochondrial function. Boxplots show the median and 25th/75th percentiles, with whiskers showing the most extreme observation less than or equal to the upper hinge  $+ 1.5 \times$  inter-quartile range. Interestingly, A01, A06 and A11 all show normal levels of TMRE staining, suggesting a specific effect on mitochondrial motility rather than a more general decrease in neuronal or mitochondrial health. This cannot be said for B03 and B04 (and A10 to a lesser extent), which apparently reduce membrane potential, although additional validation with TMRE is needed to conclude that they are in fact detrimental to cell health. Of note, four of these compounds were also active in the PPAR $\gamma$  reporter assay (Figure 3c): A01 and A11 are structurally related molecules of the pyrazolo-pyrimidine family, 1-Naphthyl-PP1 and PP2, which are Src family kinase inhibitors with additional targets including TGF $\beta$  receptors and others. A06 is Phorbol myristate acetate (aka TPA, PMA). B09 is annotated as an HSP-90 inhibitor CCT-018159. 23 compounds were tested because one of the original 24 tested in Figure 3c became unavailable.



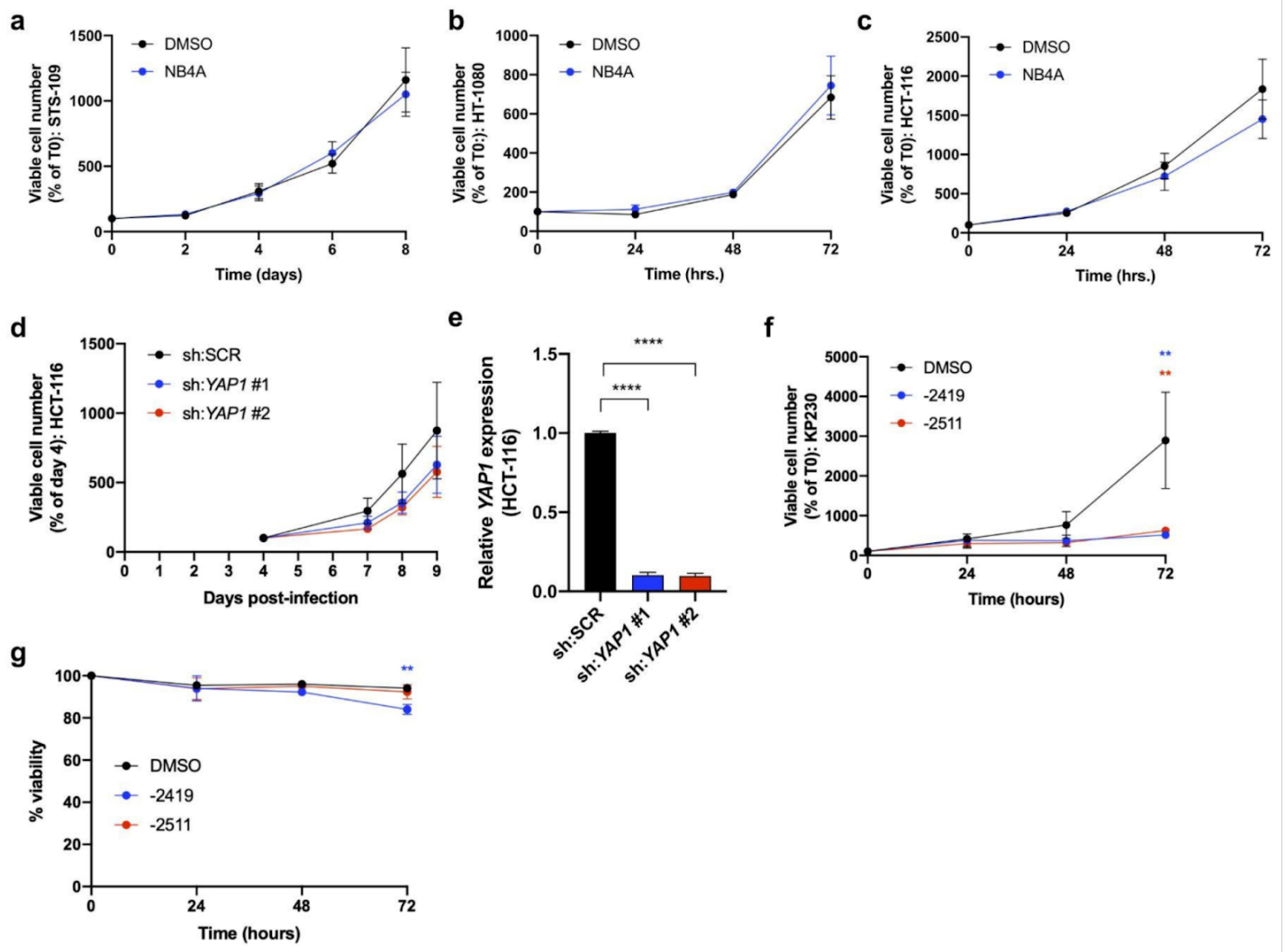
**Supplementary Figure S7: Cell Painting images related to the YAP1 pathway in U2OS cells.** Top: Cell Painting images for YAP1 overexpression compared to negative control (EMPTY, same image as in Figure 1b). Overexpressing YAP1 produces elongated cells with more cell protrusions, lower RNA staining, and disjoint, bright mitochondria patterns. Bottom: Cell Painting images for the negative control (DMSO, same image as in Figure 1b) and three compounds that correlated negatively or positively to the YAP1 overexpression profile. NB4A (BRD-K43796186) was positively correlated and the other two negatively correlated. Scale bars = 60  $\mu\text{m}$ .



**Supplementary Figure S8: Analysis of selected compounds in various YAP-related contexts.**

a) Quantification of relative levels of total YAP1 and phospho-YAP1 in H9 hPSCs after treatment with DMSO or NB4A for 24 hours.  $**P < 0.01$ ;  $***P < 0.001$  (Two-tailed student's t-test). Mean  $\pm$  SD.  $n = 3$  biologically independent experiments. A representative example western blot is shown in Figure 4c. b) A TEAD luciferase reporter was co-transfected with or without a Yap expression construct into HEK293T cells followed by treatment for 48 hours with DMSO or the indicated compounds, which appear to have no effect. The data shown are the average of three samples within a representative experiment  $\pm$  SEM. c-f) BRD-K34692511 upregulates YAP1 and target-gene mRNA levels in murine periosteal cells: c, d) YAP1 and Cyr61 mRNA levels

*in murine periosteal cells after 48 hours of treatment with BRD-K34692511 (K34) in the presence or absence of doxycycline-induced YAP<sup>S127A</sup>. e, f) YAP1 and Cyr61 mRNA levels after 1 and 4 hours of treatment. Gene expression was evaluated by one and two-way ANOVA with Tukey post hoc test n=3/group/time-point. \* indicates p<0.05 compared to untreated controls. g) BRD-K28862419 and BRD-K34692511 did not dramatically impact mRNA levels of Hippo pathway members in hPSCs. Relative transcript levels of YAP1, CTGF, and CYR61 from H9 hPSCs treated with DMSO, BRD-K28862419, or BRD-K34692511 for 24 hrs. Error bars represent mean + SEM, from n=3 independent biological replicates (one-way ANOVA with Dunnett multiple comparison test).*



**Supplementary Figure S9: Predicted YAP1-related compounds impact proliferation in a cell type-specific manner.** a, b) Growth curves of YAP1-dependent human sarcoma cells<sup>41,43</sup> treated with 10  $\mu$ M NB4A or DMSO control. c) Growth curve of HCT-116 colon cancer cells treated with 10  $\mu$ M NB4A or DMSO control. a-c are not significantly different at any time point (2-way ANOVA with Sidak's multiple comparisons test).  $n = 3$ . Mean  $\pm$  SEM. d) Growth curve of HCT-116 cells infected with YAP1-targeting shRNAs or scrambled shRNA control (sh:SCR); no conditions were significantly different at any time point (vs. sh:SCR; 2-way ANOVA with Dunnett's multiple comparisons test).  $n = 3$ . Mean  $\pm$  SEM. e) Relative YAP1 expression in the cells depicted in panel d \*\*\*\* $P < 0.0001$  vs. sh:SCR (1-way ANOVA with Dunnett's multiple comparisons test).  $n = 3$ . Mean  $\pm$  SEM. f) Growth curves of KP230 cells treated with 10  $\mu$ M BRD-K28862419, BRD-K34692511, or DMSO control. \*\* $P < 0.01$  vs. DMSO (72 hrs.; 2-way ANOVA with Dunnett's multiple comparisons test).  $n = 2$  Mean  $\pm$  SEM. g) Percent viability of KP230 cells depicted in panel f \*\* $P < 0.01$  vs. DMSO (72 hrs.; 2-way ANOVA with Dunnett's multiple comparisons test).  $n = 3$ . Mean  $\pm$  SEM. For panels a, b, c, f, and g, cells were treated with 10  $\mu$ M of the indicated inhibitor daily for 72 hours.

## Supplementary tables

**Supplementary Table S1: Top 1% correlated compound pairs are nearly 4 times more enriched in sharing a common MOA compared to the remainder of pairs.** Odds ratio is 3.95 and p-value  $< 2.2 \times 10^{-16}$  in the one sided Fisher's test.

---

	share a common MOA	have distinct MOAs
top 1% connections	161	4,234
the remainder of connections	4,147	430,911

---



**Supplementary Table S2: Gene-compound pairs which have morphological profiles with absolute correlation of at least 0.35 are around 2.5 more enriched in being relevant and trustworthy compared to the remainder of the pairs.** Odds ratio is 2.47 and p-value = 0.007 in the one sided Fisher's test. Note that this table (with 12 successful pairs, top left) considers all gene-compound pairs and reports the enrichment of strongest pairs; while in the case of the six genes reported in the main text, we examine compound matches for *each* gene.

---

	<b>Gene is among the compound targets</b>	<b>Gene is not among the compound targets</b>
$ \text{corr.}  \geq 0.35$	12	6,587
$ \text{corr.}  < 0.35$	55	74,559

---

**Supplementary Table S3: Genes sorted based on the relevance of their compound matches.**

These genes are spread across various signaling pathways and processes including mTOR, Circadian Rhythm, NF- $\kappa$ B, MAPK, WNT, Cell Cycle, and cytoskeletal reorganization.

---

	<b>Gene symbol</b>	<b>Pathway</b>	<b>adjusted p-value</b>
1	AKT1S1	TOR	0
2	CRY1	Canonical Circadian Rhythm	0
3	RELB	Canonical NF $\kappa$ B	0
4	CSNK1E	Canonical Circadian Rhythm	0.0047
5	DDIT3	Canonical ER Stress/UPR	0.0139
6	KRAS	RTK	0.0234
7	RHOA	Canonical Cytoskeletal Re-org	0.0234
8	GSK3B	Canonical WNT	0.0357
9	TCF4	Canonical WNT	0.0357
10	CCND1	Canonical Cell Cycle	0.0415

11	MAPK14	Canonical MAPK	0.0415
12	TRAF5	Canonical NFkB	0.0415
13	CDKN1A	Canonical Cell Cycle	0.0605
14	PRKCZ	Canonical PKC	0.0605
15	RAF1	Canonical MAPK	0.0605
16	BRAF	Canonical MAPK	0.0749
17	PRKACA	Canonical PKA	0.0749
18	SMAD4	Canonical SMAD	0.0749
19	PPARGC1A	Mitochondria Oxidative Phosphorylation	0.0983
20	STK3	Canonical Hippo	0.0983
21	CDK2	Canonical Cell Cycle	0.1235
22	DVL3	Canonical WNT	0.1235

23	MAP3K2	Canonical MAPK	0.1235
24	STK11	Canonical TOR	0.1235
25	TRAF2	Canonical NFkB	0.1235
26	DIABLO	Canonical Apoptosis	0.125
27	ELK1	Canonical MAPK	0.1332
28	AKT3	Canonical PI3K/AKT	0.1788
29	CDC42	Canonical Cytoskeletal Re-org	0.1788
30	EIF4EBP1	Canonical TOR	0.1788
31	MLST8	Canonical TOR	0.1788
32	PTEN	Canonical PI3K/AKT	0.1788
33	RAC1	Canonical Cytoskeletal Re-org	0.1788
34	SDHA	Canonical Hypoxia	0.1788

35	SMURF2	Canonical SMAD	0.1788
36	YAP1	Canonical Hippo	0.1788
37	NFKB1	Canonical NFkB	0.2321
38	REL	Canonical NFkB	0.2321
39	TGFB1	Canonical TGFbeta	0.2321
40	PRKCE	Canonical PKC	0.2356
41	ATF4	Canonical ER Stress/UPR	0.3377
42	BCL2L11	Apoptosis	0.3377
43	PIK3R1	Canonical PI3K/AKT	0.3377
44	AKT1	Canonical PI3K/AKT	0.3665
45	ARAF	Canonical MAPK	0.3665
46	PRKACG	PKA	0.3665

47	MAP2K4	Canonical MAPK	0.3944
48	SGK3	Canonical TOR	0.3944
49	GLI1	Hedgehog	0.4041
50	GRB10	Canonical Insulin Receptor Signaling	0.4115
51	JUN	Canonical MAPK	0.4115
52	PKIA	PKA	0.4115
53	RPS6KB1	Canonical TOR	0.4115
54	RBPJ	NOTCH	0.4355
55	MAP2K3	Canonical MAPK	0.4982
56	ATF6	ER Stress/UPR	0.5447
57	SMO	Hedgehog	0.5447
58	XBP1	Canonical ER Stress/UPR	0.614

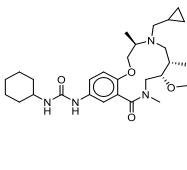
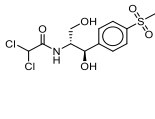
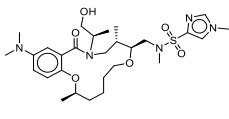
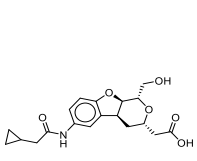
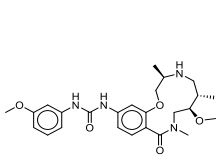
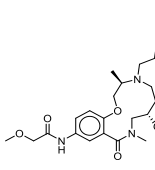
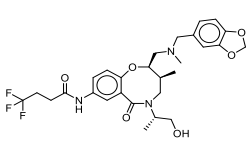
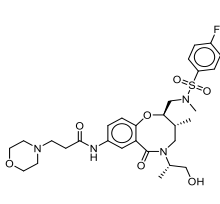
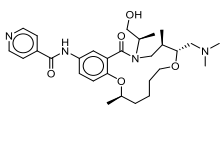
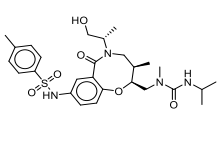
59	CEBPA	Transcription Factors	1
60	FOXO1	Canonical PI3K/AKT	1
61	HSP90B1	Canonical ER Stress/UPR	1
62	HSPA5	Canonical ER Stress/UPR	1
63	SMAD3	Canonical SMAD	1

---

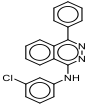
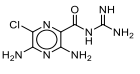
# Supplementary Table S4: GSK3 assay data and compound structures, as described in Methods

Compound ID	Compound Name	SMILES	Structure	GSK3a IC <sub>50</sub> , μM	GSK3b IC <sub>50</sub> , μM	GSK3a selectivity ratio	Note
BRD-K00760705-001-05-1	BRD0705	<chem>CC(C@@)1(c2c[nH]nc2NC2=C1C(=O)C(C)(C)C2)c1cccc1</chem>		0.131	1.05	8.04	Control
BRD-K21263731-001-06-7	BRD3731	<chem>CC(C)(C)Cc1[nH]nc2NC3=C(C(=O)CC(C)(C)C3)[C@@](C)(c12)c1ccc</chem>		0.145	0.0109	0.07	Control
BRD-K87550320-001-04-0	BRD0320	<chem>CC1(C)CC(=O)C2=C(C1)Nc1n[nH]c(C3C(C)C3)1[C@@]2(C)c1cccc(F)c1</chem>		0.00828	0.00338	0.41	Control
BRD-K16189898-001-12-8	Chiron 99021	<chem>Cc1c[nH]c(n1)-c1cnc(NCCNc2ccc(cn2)C#N)nc1-c1ccc(Cl)cc1Cl</chem>		0.00294	0.00176	0.60	Control
BRD-K55000304-001-11-9	GW8510	<chem>O=C1Nc2ccc3ncsc3c2\C1=C(Nc1cccc(cc1)S(=O)(=O)Nc1ccccn1</chem>		0.00710	0.00432	0.61	Control
BRD-K59184148-001-23-2	SB 216763	<chem>Cn1cc(C2=C(C(=O)NC2=O)c2ccc(Cl)cc2Cl)c2cccc12</chem>		0.00424	0.00554	1.31	Control
BRD-K26994486-001-01-0		<chem>C[C@@H](CO)N1C[C@H](C)[C@@H](C)[C@@H](CN(C)C(=O)Nc2c(C)noc2C)OCCCC[C@@H](C)Oc2ccc(cc2C1=O)N(C)C</chem>		2.20	35.0	15.89	active GSK3a
BRD-K91354313-001-01-6		<chem>CCC(=O)Nc1ccc2OC[C@H](C)N(C)[C@@H](C)[C@@H](CN(C)C(=O)c2c1)OC(C)=O</chem>		2.48	35.0	14.12	active GSK3a
BRD-K02827191-001-02-4		<chem>C[C@@H](CO)N1C[C@@H](C)[C@@H](CN(C)C(=O)Oc2ncc(c2C1=O)C#Cc1ccc(F)cc1</chem>		3.80	35.0	9.21	active GSK3a
BRD-K52043064-001-01-3		<chem>CO[C@@H]1CN(C)C(=O)c2ccc(NC(=O)CN(C)C)cc2OC[C@@H](C)N(C)[C@H]1C(C(=O)C1)CCCC1</chem>		3.80	35.0	9.21	active GSK3a
BRD-A62505706-001-03-1	Edoxudine	<chem>CCc1cn(C2O)C(O)C2CO)c(=O)nc1O</chem>		11.0	35.0	3.18	borderline active GSK3a
BRD-K50011338-001-01-2		<chem>CO[C@@H]1CN(C)C(=O)c2ccc(NC(=O)Nc3cccc3)cc2OC[C@@H](C)N(C)[C@H]1C(C)C(=O)C</chem>		11.0	35.0	3.18	borderline active GSK3a

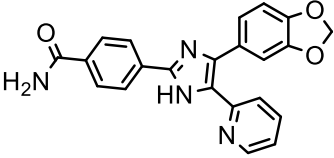
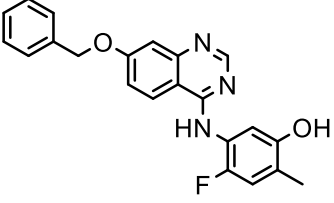
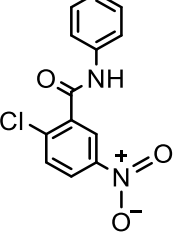
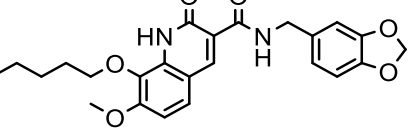
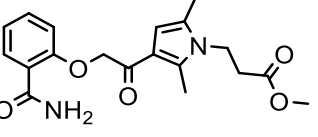
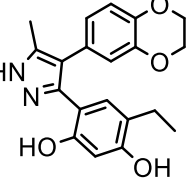


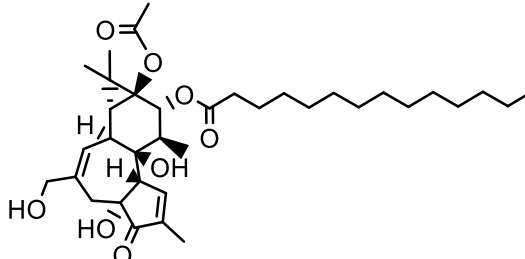
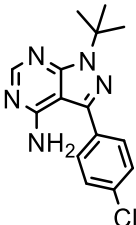
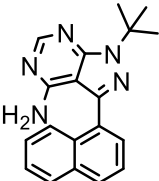
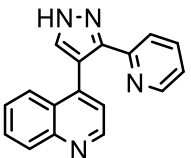
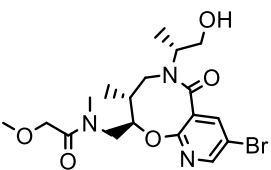
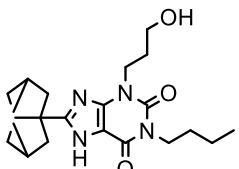
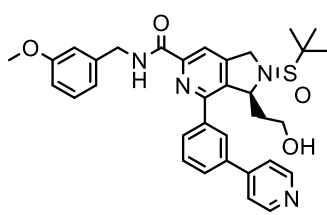
BRD-K87995704-001-01-9		<chem>CO[C@@H]1CN(C)C(=O)c2cc(NC(=O)NC3CCCCC3)ccc2OC[C@@H](C)N(CCC2CC2)C[C@@H]1C</chem> 	25.5	35.0	1.37
BRD-K79711234-001-11-8	Thiamphenicol	<chem>CS(=O)(=O)c1ccc(cc1)[C@@H](O)[C@@H](CO)N(C=O)C(Cl)Cl</chem> 	27.0	30.6	1.13
BRD-K87264606-001-01-9		<chem>C[C@H](CO)N1C[C@H](C)[C@@H](C)N(C)S(=O)(=O)c2cn(C)cn2)OCCCC[C@@H](C)Oc2c(ccc2C1=O)N(C)C</chem> 	30.0	30.0	1.00
BRD-K04407772-001-01-2		<chem>OC[C@@H]1O[C@H](CC(O)=O)C[C@@H]2[C@H]1Oc1ccc(NC(=O)CC3CC3)cc21</chem> 	35.0	35.0	1.00
BRD-K30491662-001-01-7		<chem>CO[C@H]1CNC(=O)c2ccc(NC(=O)Nc3cccc(OC)c3)cc2OC[C@@H](C)NC[C@@H]1C</chem> 	35.0	35.0	1.00
BRD-K50710722-001-01-3		<chem>CCCN1C[C@H](C)[C@@H](CN(C)C)=O)c2cc(NC(=O)COC)ccc2OC[C@H]1C</chem> 	35.0	35.0	1.00
BRD-K54148510-001-01-8		<chem>C[C@@H](CO)N1C[C@H](C)[C@@H](C)N(C)Cc2ccc3OCoc3c2)Oc2ccc(NC(=O)CCC(F)(F)F)c2C1=O</chem> 	35.0	35.0	1.00
BRD-K68074655-001-01-5		<chem>C[C@@H](CO)N1C[C@@H](C)[C@@H](CN(C)S(=O)(=O)c2ccc(F)cc2)Oc2cc(NC(=O)CCN3CCOCC3)cc2C1=O</chem> 	35.0	35.0	1.00
BRD-K68303333-001-01-8		<chem>C[C@H](CO)N1C[C@H](C)[C@@H](C)N(C)OCCC[C@H](C)Oc2ccc(NC(=O)c3ccncc3)cc2C1=O</chem> 	35.0	35.0	1.00
BRD-K80298065-001-01-8		<chem>CC(C)NC(=O)N(C)C[C@H]1Oc2ccc(NS(=O)(=O)c3cc(C)cc3)cc2C(=O)N(C)[C@@H]1C</chem> 	35.0	35.0	1.00

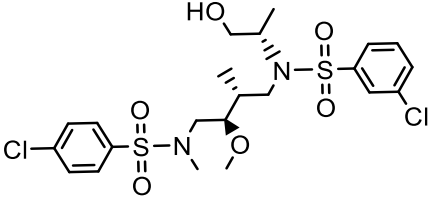
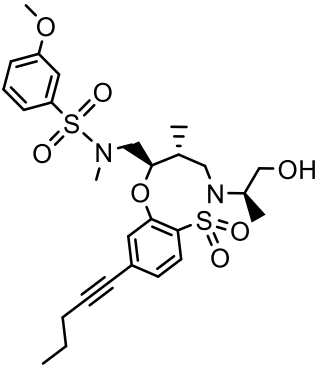
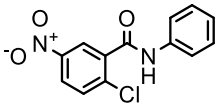
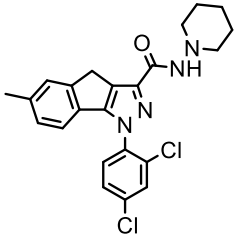
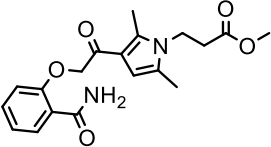
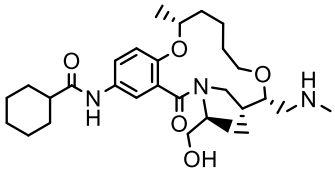
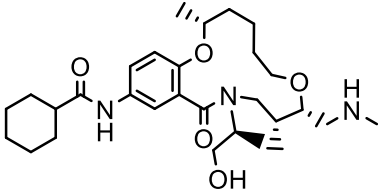
BRD-K84480302-001-01-1		<chem>C[C@@H](CO)N1[C@@H](C)C[C@@H](CN(C)C2CC2)Oc2ccc(NS(=O)(=O)c3cn(C)cn3)cc2C1=O</chem>	35.0	35.0	1.00	
BRD-K88156935-001-01-8		<chem>C[C@@H](CO)N1[C@@H](C)C[C@@H](N(C)C(=O)Nc2ccc(F)cc2)Oc2ccc(cc2C1=O)N(C)C</chem>	35.0	35.0	1.00	
BRD-K93051667-001-01-8		<chem>CO[C@@H](CN(C)C(=O)c2ccc(NS(=O)(=O)c3cn(C)cn3)cc2OC[C@@H](C)N(C)c2ccc(F)cc2)C[C@@H]1C</chem>	35.0	35.0	1.00	
BRD-K99195544-001-01-6		<chem>CCC(=O)Nc1ccc2c(OC[C@@H](C)N(C)C[C@@H](C)C[C@@H](CN(C)C2=O)OC)C(=O)CN2CCOC2)c1</chem>	35.0	35.0	1.00	
BRD-A01636364-003-08-6	Bupivacaine hydrochloride	<chem>CCCCN1CCC(CC1)C(=O)Nc1ccc(C)cc1</chem>	35.0	35.0	1.00	
BRD-A31916785-103-01-0	Timolol maleate	<chem>CC(C)C)NCC(O)COc1nsc1N1CCOCC1</chem>	35.0	35.0	1.00	
BRD-K00662280-001-01-1	CL 218872	<chem>Cc1nnc2ccc(nn12)-c1ccc(c1)C(F)(F)F</chem>	35.0	11.0	0.31	borderline active GSK3b
BRD-K30984264-001-06-2	Harmine	<chem>COc1ccc2c(c1)[nH]c1c(C)nccc21</chem>	35.0	35.0	1.00	
BRD-K37270826-001-03-7	Mifepristone	<chem>CC#C[C@]1(O)CC[C@H]2[C@@H]3CC(C4=CC(=O)CC4=C3[C@@H](C)C@]12)C)c1ccc(cc1)N(C)C</chem>	35.0	35.0	1.00	
BRD-K50388907-001-15-5	Fenofibrate	<chem>CC(C)OC(=O)C(C)C(=O)c1ccc(Cl)cc1</chem>	35.0	35.0	1.00	
BRD-K59419204-001-01-9	AM 281	<chem>Cc1c(nn(c1-c1ccc(Cl)cc1)-c1ccc(Cl)cc1)C(=O)NN1CCOCC1</chem>	35.0	35.0	1.00	
BRD-K79684402-300-01-0	Ro 10-5824	<chem>Cc1ncc(CN2CCC(=CC2)c2cccc2)c(N)n1</chem>	35.0	35.0	1.00	
BRD-K84358317-001-01-2		<chem>CC(C)C#Cc1ccc2c(O[C@@H](CN(C)C(=O)c3cnc3)C[C@@H](C)CN(C)C(=O)S2(=O)=O)c1</chem>	35.0	35.0	1.00	
BRD-K97564742-103-01-9	Mepyramine maleate	<chem>COc1ccc(cc1)CN(CCN(C)C)c1cccnc1</chem>	35.0	35.0	1.00	
BRD-K33710385-001-05-4	Ethionamide	<chem>CCc1cc(ccn1)C(N)=S</chem>	38.0	38.0	1.00	

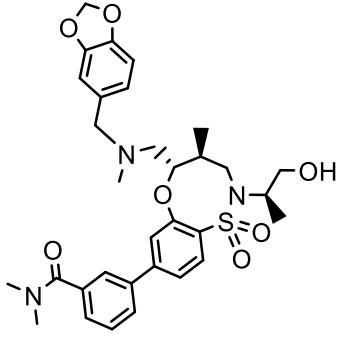
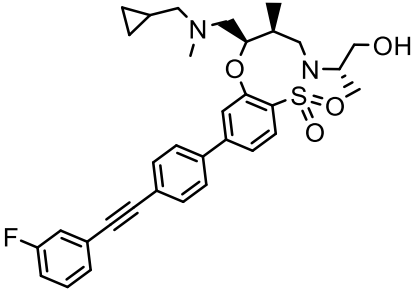
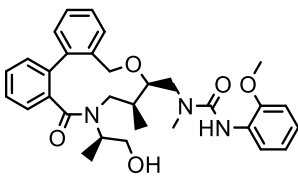
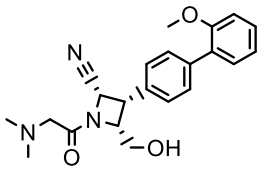
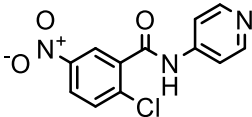
BRD-K90524085-001-05-2	MY-5445	<chem>Clc1cccc(Nc2nc(-c3cccc3)c3cccc23)c1</chem> 	50.0	33.8	0.68
BRD-K97181089-001-02-7	Amiloride	<chem>NC(=N)NC(=O)c1nc(Cl)c(N)nc1N</chem> 	75.0	75.0	1.00

**Supplementary Table S5: PGC-1 $\alpha$ -related compound structures, whose behavior is shown in Figure 3c and Supplementary Figure 5**

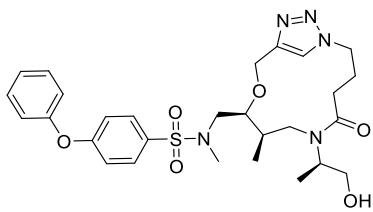
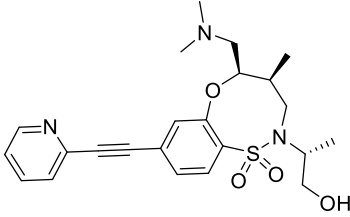
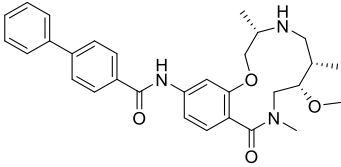
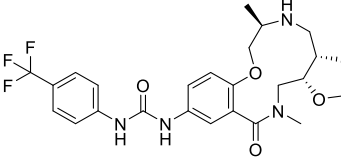
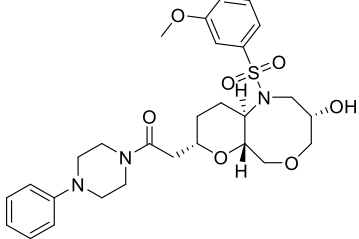
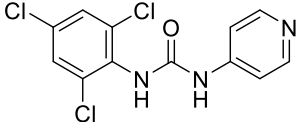
Compound ID	Structure	Name
BRD-K6729886 5		4-(4-(benzo[d][1,3]dioxol-5-yl)-5-(pyridin-2-yl)-1H-imidazol-2-yl)benzamide
BRD-K6783136 4		5-((7-(benzyloxy)quinazolin-4-yl)amino)-4-fluoro-2-methylphenol
BRD-K9325869 3		2-chloro-5-nitro-N-phenylbenzamide
BRD-K6315072 6		n-(1,3-benzodioxol-5-ylmethyl)-1,2-dihydro-7-methoxy-2-oxo-8-(pentyloxy)-3-quinolinecarboxamide
BRD-K1953488 0		methyl 3-(3-(2-(2-carbamoylphenoxy)acetyl)-2,5-dimethyl-1H-pyrrol-1-yl)propanoate
BRD-K6550312 9		4-[4-(2,3-dihydro-1,4-benzodioxin-6-yl)-5-methyl-1H-pyrazol-3-yl]-6-ethylbenzene-1,3-diol

<p>BRD- K6855212 5</p>		<p>12-O-Tetradecanoylphorbol-13-acetate</p>
<p>BRD- K9578553 7</p>		<p>1-(tert-butyl)-3-(4-chlorophenyl)-1H-pyrazolo[3,4-d]pyrimidin-4-amine</p>
<p>BRD- K2954262 8</p>		<p>1-(tert-Butyl)-3-(naphthalen-1-yl)-1H-pyrazolo[3,4-d]pyrimidin-4-amine</p>
<p>BRD- K0623429 3</p>		<p>4-(3-(pyridin-2-yl)-1H-pyrazol-4-yl)quinoline</p>
<p>BRD- K0286200 4</p>		<p><i>N</i>-[[<i>(2R,3R)</i>-8-bromo-5-[[<i>(2R)</i>]-1-hydroxypropan-2-yl]-3-methyl-6-oxo-3,4-dihydro-2<i>H</i>-pyrido[2,3-<i>b</i>][1,5]oxazocin-2-yl]methyl]-2-methoxy- <i>N</i>-methylacetamide</p>
<p>BRD- A7040746 8</p>		<p>1-butyl-3-(3-hydroxypropyl)-8-(3-tricyclo[3.3.1.0<sup>3,7</sup>]nonanyl)-7<i>H</i>-purine-2,6-dione</p>
<p>BRD- K7409480 0</p>		<p>(<i>3S</i>)-2-[[<i>(S)</i>]-<i>tert</i>-butylsulfinyl]-3-(2-hydroxyethyl)-<i>N</i>-[(3-methoxyphenyl)methyl]-4-(3-pyridin-4-ylphenyl)-1,3-dihydropyrrolo[3,4-<i>c</i>]pyridine-6-carboxamide</p>

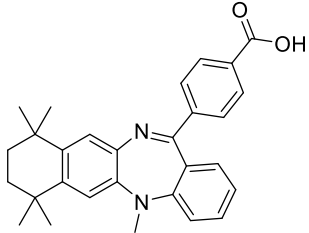
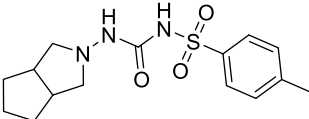
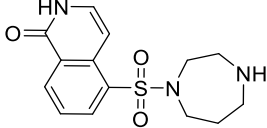
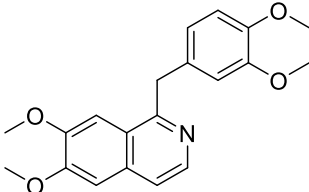
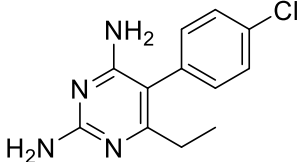
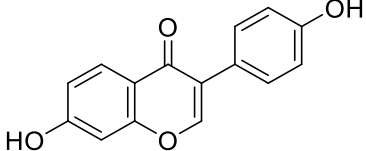
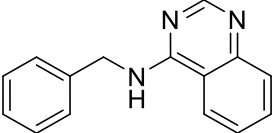
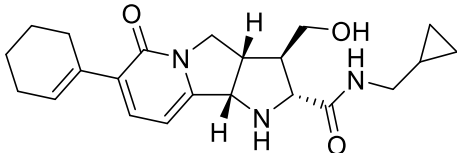
<p>BRD- K6970575 6</p>		<p>3-chloro-<i>N</i>-((2<i>R</i>,3<i>R</i>)-4-((4-chloro-<i>N</i>-methylphenyl)sulfonamido)-3-methoxy-2-methylbutyl)-<i>N</i>-((<i>S</i>)-1-hydroxypropan-2-yl)benzenesulfonamide</p>
<p>BRD- K1713364 2</p>		<p><i>N</i>-(((4<i>R</i>,5<i>R</i>)-2-((<i>R</i>)-1-hydroxypropan-2-yl)-4-methyl-1,1-dioxido-8-(pent-1-yn-1-yl)-2,3,4,5-tetrahydrobenzo[<i>b</i>][1,4,5]oxathiazocin-5-yl)methyl)-3-methoxy-<i>N</i>-methylbenzenesulfonamide</p>
<p>BRD- K1044993 8</p>		<p>3-chloro-<i>N</i>-[(2<i>R</i>,3<i>R</i>)-4-[(4-chlorophenyl)sulfonylmethylamino]-3-methoxy-2-methylbutyl]-<i>N</i>-[(2<i>R</i>)-1-hydroxypropan-2-yl]benzenesulfonamide</p>
<p>BRD- K3545807 9</p>		<p>5-methyl-2-phenyl-4<i>H</i>-pyrazol-3-one</p>
<p>BRD- K6528570 0</p>		<p>1-(2,4-dichlorophenyl)-6-methyl-<i>N</i>-piperidin-1-yl-4<i>H</i>-indeno[1,2-<i>c</i>]pyrazole-3-carboxamide</p>
<p>BRD- K1953488 0</p>		<p>methyl 3-[3-[2-(2-carbamoylphenoxy)acetyl]-2,5-dimethylpyrrol-1-yl]propanoate</p>
<p>BRD- K4514247 2</p>		<p><i>N</i>-[(3<i>R</i>,9<i>S</i>,10<i>R</i>)-12-[(2<i>S</i>)-1-hydroxypropan-2-yl]-3,10-dimethyl-9-(methylaminomethyl)-13-oxo-2,8-dioxo-12-azabicyclo[12.4.0]octadeca-</p>

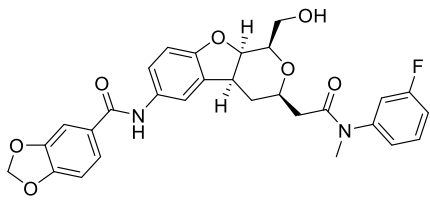
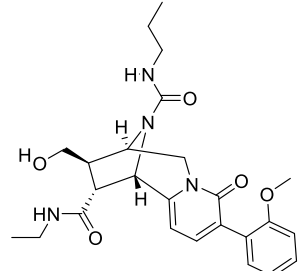
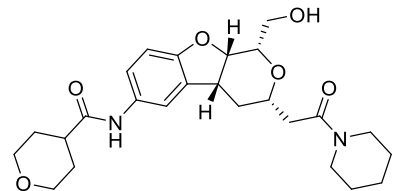
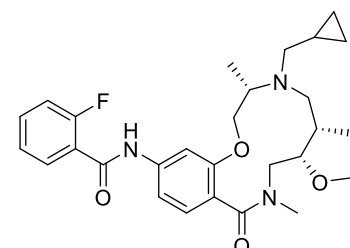
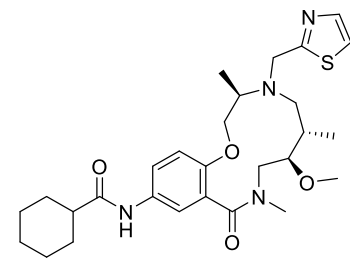
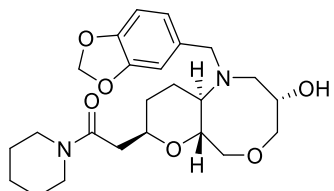
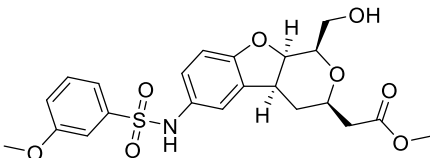
		1(14),15,17-trien-16-yl]cyclohexanecarboxamide
BRD-K6822395 4		3-((4S,5S)-5-(((benzo[d][1,3]dioxol-5-ylmethyl)(methylamino)methyl)-2-((R)-1-hydroxypropan-2-yl)-4-methyl-1,1-dioxido-2,3,4,5-tetrahydrobenzo[b][1,4,5]oxathiazocin-8-yl)-N,N-dimethylbenzamide
BRD-K1430970 6		(4S,5R)-5-(((cyclopropylmethyl)(methylamino)methyl)-8-(4-((3-fluorophenyl)ethynyl)phenyl)-2-((S)-1-hydroxypropan-2-yl)-4-methyl-2,3,4,5-tetrahydrobenzo[b][1,4,5]oxathiazocine 1,1-dioxide
BRD-K4355616 0		1-[[[(10R,11S)-13-[(2R)-1-hydroxypropan-2-yl]-11-methyl-14-oxo-9-oxa-13-azatricyclo[13.4.0.0 <sup>2,7</sup> ]nonadeca-1(19),2,4,6,15,17-hexaen-10-yl]methyl]-3-(2-methoxyphenyl)-1-methylurea
BRD-K5960531 0		(2S,3S,4R)-1-[2-(dimethylamino)acetyl]-4-(hydroxymethyl)-3-[4-(2-methoxyphenyl)phenyl]azetidine-2-carbonitrile
T0070907 (control)		2-chloro-5-nitro-N-(pyridin-4-yl)benzamide

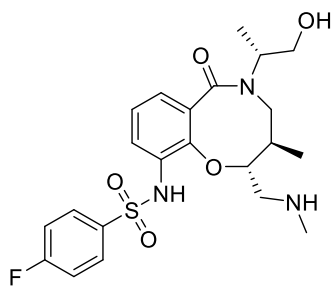
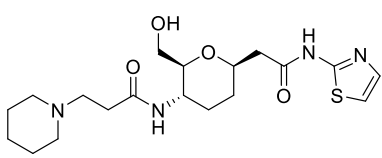
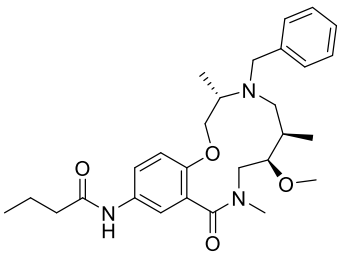
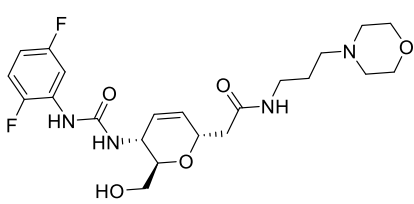
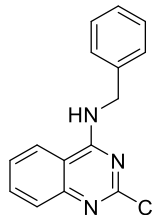
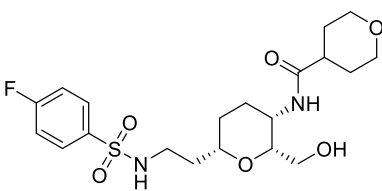
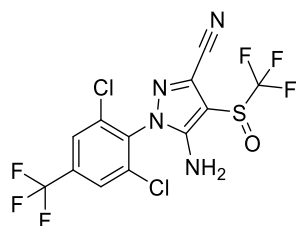
**Supplementary Table S6: YAP1-related compound structures**

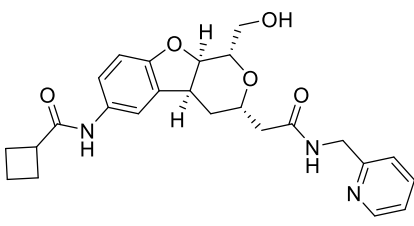
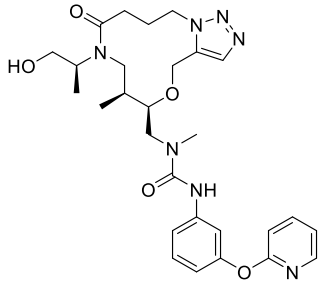
Compound ID	Structure	Name
BRD-K96698997 (Cmpd. 1)		N-[[[(8R,9S)-6-[(2R)-1-hydroxypropan-2-yl]-8-methyl-5-oxo-10-oxa-1,6,13,14-tetrazabicyclo[10.2.1]pentadeca-12(15),13-dien-9-yl)methyl]-N-methyl-4-phenoxybenzenesulfonamide
BRD-K13719685 (Cmpd. 2)		(4S,5R)-5-((dimethylamino)methyl)-2-((R)-1-hydroxypropan-2-yl)-4-methyl-8-(pyridin-2-ylethynyl)-2,3,4,5-tetrahydrobenzo[b][1,4,5]oxathiazocine 1,1-dioxide
BRD-K34692511 (Cmpd. 3)		N-[(4S,7S,8S)-8-methoxy-4,7,10-trimethyl-11-oxo-2-oxa-5,10-diazabicyclo[10.4.0]hexadeca-1(12),13,15-trien-15-yl]-4-phenylbenzamide
BRD-K28862419 (Cmpd. 4)		1-[(4R,7S,8S)-8-methoxy-4,7,10-trimethyl-11-oxo-2-oxa-5,10-diazabicyclo[10.4.0]hexadeca-1(12),13,15-trien-14-yl]-3-[4-(trifluoromethyl)phenyl]urea
BRD-K70003473 (Cmpd. 5)		2-[(3S,6aR,8S,10aR)-3-hydroxy-1-(3-methoxyphenyl)sulfonyl-3,4,6,6a,8,9,10,10a-octahydro-2H-pyrano[2,3-c][1,5]oxazocin-8-yl]-1-(4-phenyl-1-piperazinyl)ethanone
BRD-K46678324 (Cmpd. 6)		1-pyridin-4-yl-3-(2,4,6-trichlorophenyl)urea



<p>BRD- K06593056 (Cmpd. 7)</p>		<p>4-(5,7,7,10,10-pentamethyl-8,9-dihydronaphtho[2,3-b][1,4]benzodiazepin-13-yl)benzoic acid</p>
<p>BRD- A61154809 (Cmpd. 8)</p>		<p>1-(3,3a,4,5,6,6a-hexahydro-1H-cyclopenta[c]pyrrol-2-yl)-3-(4-methylphenyl)sulfonylurea</p>
<p>BRD- K77793136 (Cmpd. 9)</p>		<p>5-(1,4-diazepan-1-ylsulfonyl)-2H-isoquinolin-1-one</p>
<p>BRD- K15567136 (Cmpd. 10)</p>		<p>1-[(3,4-dimethoxyphenyl)methyl]-6,7-dimethoxyisoquinoline</p>
<p>BRD- K88429204 (Cmpd. 11)</p>		<p>5-(4-chlorophenyl)-6-ethylpyrimidine-2,4-diamine</p>
<p>BRD- K42095107 (Cmpd. 12)</p>		<p>7-hydroxy-3-(4-hydroxyphenyl)chromen-4-one</p>
<p>BRD- K43796186 (Cmpd. 13)</p>		<p>N-benzylquinazolin-4-amine</p>
<p>BRD- K37451830 (Cmpd. 14)</p>		<p>(2R,3R,3aS,9bS)-7-(1-cyclohexenyl)-N-(cyclopropylmethyl)-3-(hydroxymethyl)-6-oxo-1,2,3,3a,4,9b-hexahydropyrrolo[2,3-a]indolizine-2-carboxamide</p>

<p>BRD- K03953354 (Cmpd. 15)</p>		<p>N-[(1R,3R,4aS,9aR)-3-[2-[(3-fluorophenyl)methylamino]-2-oxoethyl]-1-(hydroxymethyl)-3,4,4a,9a-tetrahydro-1H-pyrano[3,4-b]benzofuran-6-yl]-1,3-benzodioxole-5-carboxamide</p>
<p>BRD- K39839146 (Cmpd. 16)</p>		<p>(1S,9R,10R,11R)-11-N-ethyl-10-(hydroxymethyl)-5-(2-methoxyphenyl)-6-oxo-12-N-propyl-7,12-diazatricyclo[7.2.1.02,7]dodeca-2,4-diene-11,12-dicarboxamide</p>
<p>BRD- K62768599 (Cmpd. 17)</p>		<p>N-[(1S,3S,4aR,9aS)-1-(hydroxymethyl)-3-[2-oxo-2-(1-piperidinyl)ethyl]-3,4,4a,9a-tetrahydro-1H-pyrano[3,4-b]benzofuran-6-yl]-4-oxanecarboxamide</p>
<p>BRD- K42367391 (Cmpd. 18)</p>		<p>N-[(5S,6S,9S)-8-(cyclopropylmethyl)-5-methoxy-3,6,9-trimethyl-2-oxo-1,1-oxa-3,8-diazabicyclo[10.4.0]hexadeca-1(12),13,15-trien-14-yl]-2-fluorobenzamide</p>
<p>BRD- K22874335 (Cmpd. 19)</p>		<p>N-[(4R,7S,8R)-8-methoxy-4,7,10-trimethyl-11-oxo-5-(1,3-thiazol-2-ylmethyl)-2-oxa-5,10-diazabicyclo[10.4.0]hexadeca-1(12),13,15-trien-14-yl]cyclohexanecarboxamide</p>
<p>BRD- K41723088 (Cmpd. 20)</p>		<p>2-[(3S,6aR,8R,10aR)-1-(1,3-benzodioxol-5-ylmethyl)-3-hydroxy-3,4,6,6a,8,9,10,10a-octahydro-2H-pyrano[2,3-c][1,5]oxazocin-8-yl]-1-piperidin-1-ylethanone</p>
<p>BRD- K68530167 (Cmpd. 21)</p>		<p>2-[(1R,3R,4aS,9aR)-1-(hydroxymethyl)-6-[(3-methoxyphenyl)sulfonylamino]-3,4,4a,9a-tetrahydro-1H-pyrano[3,4-b]benzofuran-6-yl]-1,3-benzodioxole-5-carboxamide</p>

		b]benzofuran-3-yl]acetic acid methyl ester
BRD-K22754756 (Cmpd. 22)		4-fluoro-N-[(2R,3R)-5-[(2R)-1-hydroxypropan-2-yl]-3-methyl-2-(methylaminomethyl)-6-oxo-3,4-dihydro-2H-1,5-benzoxazocin-10-yl]benzenesulfonamide
BRD-K11266478 (Cmpd. 23)		N-[(2S,3S,6R)-2-(hydroxymethyl)-6-[2-oxo-2-(1,3-thiazol-2-ylamino)ethyl]oxan-3-yl]-3-piperidin-1-ylpropanamide
BRD-K00135177 (Cmpd. 24)		N-[(4S,7R,8R)-8-methoxy-4,7,10-trimethyl-11-oxo-5-(phenylmethyl)-2-oxa-5,10-diazabicyclo[10.4.0]hexadeca-1(12),13,15-trien-14-yl]butanamide
BRD-K40143134 (Cmpd. 25)		2-[(2R,3R,6S)-3-[[2,5-difluoroanilino]-oxomethyl]amino]-2-(hydroxymethyl)-3,6-dihydro-2H-pyran-6-yl]-N-[3-(4-morpholinyl)propyl]acetamide
BRD-K11758216 (Cmpd. 26)		N-benzyl-2-chloroquinazolin-4-amine
BRD-K48052543 (Cmpd. 27)		N-[(2R,3S,6S)-6-[2-[(4-fluorophenyl)sulfonylamino]ethyl]-2-(hydroxymethyl)oxan-3-yl]oxane-4-carboxamide
BRD-A50675702 (Cmpd. 28)		5-amino-1-[2,6-dichloro-4-(trifluoromethyl)phenyl]-4-(trifluoromethyl)sulfinyl-1H-pyrazole-3-carbonitrile

<p>BRD- K28043081 (Cmpd. 29)</p>		<p>N-[(1S,3S,4aS,9aR)-1-(hydroxymethyl)-3-[2-oxo-2-(pyridin-2-ylmethylamino)ethyl]-3,4,4a,9a-tetrahydro-1H-pyrano[3,4-b][1]benzofuran-6-yl]cyclobutanecarboxamide</p>
<p>BRD- K19969618 (Cmpd. 30)</p>		<p>1-[[[(8S,9R)-6-[(2S)-1-hydroxypropan-2-yl]-8-methyl-5-oxo-10-oxa-1,6,14,15-tetrazabicyclo[10.3.0]pentadeca-12,14-dien-9-yl]methyl]-1-methyl-3-(3-pyridin-2-yloxyphenyl)urea</p>

**Supplementary Table S7: Thirty compounds whose Cell Painting profile matched (25 compounds) or opposed (5 compounds) the overexpression of the Hippo pathway effector Yes-associated protein 1 (YAP1)**

	Broad ID	MOA	Compound Name	Known Targets	Corr. to YAP cluster	Avg. Cell Count z-score	Corr. to TRAF2
1	BRD-K96698997-001-01-4				-0.451816097371088	-1.09876751317736	0.483378769177758
11	BRD-K88429204-001-04-7	dihydrofolate reductase inhibitor	pyrimethamine	DHFR, SLC47A1	0.450273057324876	-0.21652845532613	-0.349609799358579
9	BRD-K77793136-003-01-4	rho associated kinase inhibitor	hydroxyfasudil	PKIA, PRKACA, ROCK1	0.445765052349004	-1.05491865344321	-0.466745148730574
5	BRD-K70003473-001-01-0				-0.419476423486351	0.57275101988869	0.309863968937689
21	BRD-K68530167-001-02-5				0.493953439051083	-0.141108416583381	-0.461903561022211
17	BRD-K62768599-001-01-7				0.488328497910833	-0.739206863357278	-0.52723612634195
27	BRD-K48052543-001-01-2				0.509868432726129	0.0980140318335538	-0.413168132822434
6	BRD-K46678324-001-03-7	rho associated kinase inhibitor	RHO-kinase inhibitor II		0.428418602602677	-0.725175228242348	-0.339745295430873
13	BRD-K43796186-001-01-1	EGFR inhibitor	benzyl-quinazolin-4-yl-amine	EGFR	0.462214494435451	-0.570827241978117	-0.377843726025219
18	BRD-K42367391-001-01-3				0.488715954293843	-0.937403709355667	-0.272772324093652

	Broad ID	MOA	Compound Name	Known Targets	Corr. to YAP cluster	Avg. Cell Count z-score	Corr. to TRAF2
12	BRD-K42095107-001-02-3	estrogen receptor agonist	daidzein	ESRRA, ESRRB, ESRRG, TRPC5	0.458309143762898	-0.881277168895946	-0.371958320674078
20	BRD-K41723088-001-01-6				0.491645117137496	-0.0709502410087301	-0.43890527237543
25	BRD-K40143134-001-01-2				0.50094854898695	-0.114799100742887	-0.342751435013124
16	BRD-K39839146-001-01-4				0.483549276460743	0.218452233236704	-0.428362405612274
14	BRD-K37451830-001-01-1				0.480168234528875	-0.00429997421281192	-0.416740972979351
3	BRD-K34692511-001-01-9				-0.439820984888043	0.478037482862912	0.286882376707942
4	BRD-K28862419-001-01-9				-0.431674202259506	-2.04414892904578	0.406783833287405
29	BRD-K28043081-001-01-3				0.526963070335337	-0.553287698084454	-0.406037778061057
19	BRD-K22874335-001-01-1				0.490400094569485	-1.70388177750873	-0.362018046441038
22	BRD-K22754756-001-01-5				0.496607051682064	-1.40921744009519	-0.297027575600364
30	BRD-K19969618-001-01-2				0.548319649662317	0.77971763783391	-0.466667305651416

	Broad ID	MOA	Compound Name	Known Targets	Corr. to YAP cluster	Avg. Cell Count z-score	Corr. to TRAF2
10	BRD-K15567136-001-01-1	phosphodiesterase inhibitor	papaverine hydrochloride	PDE10A, PDE4B, PDE5A	0.44641427678599	-0.656771007057064	-0.493557215874781
2	BRD-K13719685-001-01-5				-0.442645220271481	2.10395320180544	0.359126741534968
26	BRD-K11758216-001-01-3				0.507801351616454	-1.20225082214997	-0.440615345966013
23	BRD-K11266478-001-01-0				0.498791551452305	0.485053300420377	-0.439765555665776
7	BRD-K06593056-001-01-4	retinoid receptor agonist	LE-135	RARB	0.435680365509664	-0.790948517843583	-0.451237141338472
15	BRD-K03953354-001-01-2				0.483314867234996	-1.39693975936963	-0.481607208500513
24	BRD-K00135177-001-01-4				0.500357831891246	0.400863489730796	-0.364867410280201
8	BRD-A61154809-001-03-5	ATP channel blocker insulin secretagogue	gliclazide	ABCC8, VEGFA	0.440145834465088	0.820309153702101	-0.33133766243123
28	BRD-A50675702-001-03-0	chloride channel blocker GABA gated chloride channel blocker	fipronil		0.51019424419505	-0.118808139347153	-0.475169203024327

# Supplementary Table S8: RNA-sequencing-based enrichment analysis of Hallmark gene sets up- and down-regulated in KP230 cells by NB4A

NAME	GS follow link to MsigDB	GS DETAILS	SIZE	ES	NES	NOM p-val	FDR q-val	FWER p-val	RANK AT MAX	LEADING EDGE	UPREGULATED OR DOWNREGULATED
HALLMARK_INTERFERON_ALPHA_RESPONSE	HALLMARK_INTERFERON_ALPHA_RESPONSE	Details ...	86	0.5941053	2.2873087	0	0	0	0	1819 tags=38%, list=12%, signal=43%	Upregulated in NB4A-treated
HALLMARK_INTERFERON_GAMMA_RESPONSE	HALLMARK_INTERFERON_GAMMA_RESPONSE	Details ...	166	0.3945195	1.7322907	0	0.00368626	0.008	2131	tags=29%, list=14%, signal=33%	Upregulated in NB4A-treated
HALLMARK_PROTEIN_SECRETION	HALLMARK_PROTEIN_SECRETION	Details ...	92	0.41896117	1.6522279	0.002403846	0.0096725	0.032	2513	tags=36%, list=17%, signal=43%	Upregulated in NB4A-treated
HALLMARK_MYC_TARGETS_V1	HALLMARK_MYC_TARGETS_V1	Details ...	182	0.305301	1.4714037	0.005181347	0.04932377	0.189	2181	tags=26%, list=15%, signal=30%	Upregulated in NB4A-treated
HALLMARK_APOPTOSIS	HALLMARK_APOPTOSIS	Details ...	150	0.34260988	1.4562898	0.002717391	0.04559618	0.214	1928	tags=27%, list=13%, signal=31%	Upregulated in NB4A-treated
HALLMARK_UV_RESPONSE_UP	HALLMARK_UV_RESPONSE_UP	Details ...	146	0.30856675	1.3382866	0.024523161	0.11366022	0.524	3312	tags=26%, list=22%, signal=46%	Upregulated in NB4A-treated
HALLMARK_COMPLEMENT	HALLMARK_COMPLEMENT	Details ...	158	0.29993588	1.3087488	0.036931816	0.12590155	0.617	2019	tags=20%, list=13%, signal=23%	Upregulated in NB4A-treated
HALLMARK_DNA_REPAIR	HALLMARK_DNA_REPAIR	Details ...	143	0.3008566	1.2843143	0.035326086	0.13475496	0.689	3426	tags=40%, list=23%, signal=51%	Upregulated in NB4A-treated
HALLMARK_PDK_AKT_MTOR_SIGNALING	HALLMARK_PDK_AKT_MTOR_SIGNALING	Details ...	97	0.27325217	1.1698457	0.15869917	0.30128673	0.948	2927	tags=32%, list=20%, signal=39%	Upregulated in NB4A-treated
HALLMARK_HEME_METABOLISM	HALLMARK_HEME_METABOLISM	Details ...	169	0.262995614	1.1590812	0.13533835	0.2913993	0.958	2760	tags=24%, list=18%, signal=29%	Upregulated in NB4A-treated
HALLMARK_ALLOGRAFT_REJECTION	HALLMARK_ALLOGRAFT_REJECTION	Details ...	149	0.26266745	1.1286	0.17435898	0.33088337	0.984	2168	tags=19%, list=14%, signal=22%	Upregulated in NB4A-treated
HALLMARK_OXIDATIVE_PHOSPHORYLATION	HALLMARK_OXIDATIVE_PHOSPHORYLATION	Details ...	192	0.2433627	1.0804513	0.26944444	0.42189047	0.999	3242	tags=30%, list=22%, signal=38%	Upregulated in NB4A-treated
HALLMARK_REACTIVE_OXYGEN_SPECIES_PATHWAY	HALLMARK_REACTIVE_OXYGEN_SPECIES_PATHWAY	Details ...	46	0.30948043	1.072884	0.35746607	0.4090726	0.999	2204	tags=26%, list=15%, signal=31%	Upregulated in NB4A-treated
HALLMARK_IL2_STATS_SIGNALING	HALLMARK_IL2_STATS_SIGNALING	Details ...	178	0.2425146	1.0618333	0.30357143	0.40563384	1	2168	tags=21%, list=14%, signal=24%	Upregulated in NB4A-treated
HALLMARK_IL6_JAK_STATS_SIGNALING	HALLMARK_IL6_JAK_STATS_SIGNALING	Details ...	75	0.27034676	1.0383954	0.378866	0.4350973	1	3312	tags=31%, list=22%, signal=39%	Upregulated in NB4A-treated
HALLMARK_ADIPOGENESIS	HALLMARK_ADIPOGENESIS	Details ...	189	0.22059528	1.0254962	0.3837335	0.4401859	1	2738	tags=25%, list=19%, signal=30%	Upregulated in NB4A-treated
HALLMARK_PANCREAS_BETA_CELLS	HALLMARK_PANCREAS_BETA_CELLS	Details ...	25	0.3470038	1.0112545	0.4312115	0.4494147	1	1269	tags=16%, list=8%, signal=17%	Upregulated in NB4A-treated
HALLMARK_SPERMATOGENESIS	HALLMARK_SPERMATOGENESIS	Details ...	109	0.23348868	0.9675974	0.5630027	0.53295434	1	4079	tags=33%, list=27%, signal=44%	Upregulated in NB4A-treated
HALLMARK_EPITHELIAL_MESENCHYMAL_TRANSITION	HALLMARK_EPITHELIAL_MESENCHYMAL_TRANSITION	Details ...	100	0.2642706	-2.734083	0	0	0	1536	tags=32%, list=10%, signal=47%	Downregulated in NB4A-treated
HALLMARK_ANGIOGENESIS	HALLMARK_ANGIOGENESIS	Details ...	31	-0.6635637	-2.009867	0	0	0	1291	tags=35%, list=9%, signal=39%	Downregulated in NB4A-treated
HALLMARK_GLYCOLYSIS	HALLMARK_GLYCOLYSIS	Details ...	184	-0.4841484	-2.004427	0	0	0	1519	tags=28%, list=10%, signal=31%	Downregulated in NB4A-treated
HALLMARK_UV_RESPONSE_DN	HALLMARK_UV_RESPONSE_DN	Details ...	137	-0.504841	-2.002119	0	0	0	2807	tags=40%, list=19%, signal=49%	Downregulated in NB4A-treated
HALLMARK_HYPOXIA	HALLMARK_HYPOXIA	Details ...	186	-0.4647971	-1.924311	0	1.94E-04	0.001	2715	tags=40%, list=18%, signal=48%	Downregulated in NB4A-treated
HALLMARK_APICAL_JUNCTION	HALLMARK_APICAL_JUNCTION	Details ...	185	-0.421712	-1.741695	0	0.00509011	0.029	2672	tags=32%, list=18%, signal=39%	Downregulated in NB4A-treated
HALLMARK_TGF_BETA_SIGNALING	HALLMARK_TGF_BETA_SIGNALING	Details ...	54	-0.5039986	-1.720936	0.003412969	0.005356684	0.036	1462	tags=31%, list=10%, signal=35%	Downregulated in NB4A-treated
HALLMARK_HEDGEHOG_SIGNALING	HALLMARK_HEDGEHOG_SIGNALING	Details ...	34	-0.5154501	-1.700231	0.005235602	0.005728535	0.044	3166	tags=41%, list=21%, signal=52%	Downregulated in NB4A-treated
HALLMARK_NOTCH_SIGNALING	HALLMARK_NOTCH_SIGNALING	Details ...	31	-0.5646099	-1.685015	0.010948905	0.006704273	0.055	3007	tags=45%, list=20%, signal=56%	Downregulated in NB4A-treated
HALLMARK_ESTROGEN_RESPONSE_EARLY	HALLMARK_ESTROGEN_RESPONSE_EARLY	Details ...	184	-0.3867249	-1.59521	0.00155521	0.015935246	0.142	1426	tags=20%, list=10%, signal=22%	Downregulated in NB4A-treated
HALLMARK_WNT_BETA_CATENIN_SIGNALING	HALLMARK_WNT_BETA_CATENIN_SIGNALING	Details ...	38	-0.4959761	-1.583363	0.01856716	0.015919015	0.151	3607	tags=42%, list=20%, signal=53%	Downregulated in NB4A-treated
HALLMARK_MTORC1_SIGNALING	HALLMARK_MTORC1_SIGNALING	Details ...	188	-0.3639892	-1.514257	0.00312989	0.026771887	0.269	1382	tags=21%, list=9%, signal=23%	Downregulated in NB4A-treated
HALLMARK_MYOGENESIS	HALLMARK_MYOGENESIS	Details ...	186	-0.3648306	-1.504344	0.00157632	0.02799793	0.299	1336	tags=18%, list=9%, signal=20%	Downregulated in NB4A-treated
HALLMARK_CHOLESTEROL_HOMEOSTASIS	HALLMARK_CHOLESTEROL_HOMEOSTASIS	Details ...	69	-0.4184438	-1.493341	0.028169014	0.029403457	0.333	1705	tags=30%, list=11%, signal=34%	Downregulated in NB4A-treated
HALLMARK_MITOTIC_SPINDLE	HALLMARK_MITOTIC_SPINDLE	Details ...	193	-0.3635059	-1.488942	0.010736196	0.028197076	0.341	3281	tags=36%, list=22%, signal=45%	Downregulated in NB4A-treated
HALLMARK_APICAL_SURFACE	HALLMARK_APICAL_SURFACE	Details ...	39	-0.4417995	-1.415298	0.060763888	0.049216405	0.551	2354	tags=31%, list=16%, signal=36%	Downregulated in NB4A-treated
HALLMARK_KRAS_SIGNALING_UP	HALLMARK_KRAS_SIGNALING_UP	Details ...	181	-0.3398556	-1.398792	0.017377567	0.053476032	0.61	2296	tags=23%, list=15%, signal=26%	Downregulated in NB4A-treated
HALLMARK_ESTROGEN_RESPONSE_LATE	HALLMARK_ESTROGEN_RESPONSE_LATE	Details ...	179	-0.3309946	-1.382303	0.009584654	0.05974807	0.662	1426	tags=18%, list=10%, signal=20%	Downregulated in NB4A-treated
HALLMARK_INFLAMMATORY_RESPONSE	HALLMARK_INFLAMMATORY_RESPONSE	Details ...	163	-0.3420927	-1.378404	0.002733653	0.05833988	0.675	1185	tags=16%, list=8%, signal=17%	Downregulated in NB4A-treated
HALLMARK_TNFA_SIGNALING_VIA_NFKB	HALLMARK_TNFA_SIGNALING_VIA_NFKB	Details ...	188	-0.3291668	-1.373827	0.013740458	0.05704531	0.688	1189	tags=20%, list=8%, signal=21%	Downregulated in NB4A-treated
HALLMARK_KRAS_SIGNALING_DN	HALLMARK_KRAS_SIGNALING_DN	Details ...	138	-0.3369457	-1.336891	0.051948052	0.07507158	0.807	2429	tags=19%, list=16%, signal=22%	Downregulated in NB4A-treated
HALLMARK_COAGULATION	HALLMARK_COAGULATION	Details ...	107	-0.346556	-1.28073	0.08777969	0.11387649	0.92	2896	tags=30%, list=19%, signal=37%	Downregulated in NB4A-treated
HALLMARK_UNFOLDED_PROTEIN_RESPONSE	HALLMARK_UNFOLDED_PROTEIN_RESPONSE	Details ...	103	-0.3199706	-1.226251	0.13128039	0.16439793	0.978	2247	tags=29%, list=15%, signal=34%	Downregulated in NB4A-treated
HALLMARK_G2M_CHECKPOINT	HALLMARK_G2M_CHECKPOINT	Details ...	190	-0.2905551	-1.219829	0.097826086	0.16501382	0.983	3942	tags=39%, list=26%, signal=52%	Downregulated in NB4A-treated
HALLMARK_ANDROGEN_RESPONSE	HALLMARK_ANDROGEN_RESPONSE	Details ...	91	-0.298016	-1.129188	0.21880072	0.2863506	0.999	1382	tags=19%, list=9%, signal=20%	Downregulated in NB4A-treated
HALLMARK_P53_PATHWAY	HALLMARK_P53_PATHWAY	Details ...	187	-0.2723642	-1.106566	0.25832012	0.3154989	0.999	1024	tags=14%, list=7%, signal=15%	Downregulated in NB4A-treated
HALLMARK_XENOBIOTIC_METABOLISM	HALLMARK_XENOBIOTIC_METABOLISM	Details ...	169	-0.2588365	-1.063456	0.31388012	0.38838965	0.999	1382	tags=14%, list=9%, signal=15%	Downregulated in NB4A-treated
HALLMARK_MYC_TARGETS_V2	HALLMARK_MYC_TARGETS_V2	Details ...	54	-0.2797416	-0.968363	0.4856661	0.59060425	1	3804	tags=37%, list=25%, signal=49%	Downregulated in NB4A-treated
HALLMARK_FATTY_ACID_METABOLISM	HALLMARK_FATTY_ACID_METABOLISM	Details ...	148	-0.2398035	-0.964624	0.53543305	0.58000576	1	2867	tags=24%, list=19%, signal=29%	Downregulated in NB4A-treated
HALLMARK_E2F_TARGETS	HALLMARK_E2F_TARGETS	Details ...	192	-0.2091263	-0.868751	0.8031496	0.7996806	1	2856	tags=25%, list=19%, signal=31%	Downregulated in NB4A-treated
HALLMARK_PEROXISOME	HALLMARK_PEROXISOME	Details ...	90	-0.2161393	-0.804066	0.84477127	0.902477	1	1405	tags=12%, list=9%, signal=13%	Downregulated in NB4A-treated
HALLMARK_BILE_ACID_METABOLISM	HALLMARK_BILE_ACID_METABOLISM	Details ...	98	-0.2020332	-0.754092	0.93811077	0.9386531	1	1464	tags=13%, list=10%, signal=15%	Downregulated in NB4A-treated



**Supplementary Table S9: RT-qPCR primer sequences used in the study.**

<b>Gene name</b>	<b>Forward primer</b>	<b>Reverse primer</b>
<i>GAPDH</i>	GTGGTCTCCTCTGACTTCAAC	CCTGTTGCTGTAGCCAAATTC
<i>YAP1</i>	GCTGCCACCAAGCTAGATAA	GTGCATGTGTCTCCTTAGATCC
<i>CTGF</i>	GTGCATCCGTACTIONCCAAA	CTCCACAGAATTTAGCTCGGTAT
<i>CYR61</i>	AGCCTCGCATCCTATACAACC	TTCTTTCACAAGGCGGCACTC
<i>Yap1</i>	GATGTCTCAGGAATTGAGAAC	CTGTATCCATTTTCATCCACAC
<i>Cyr61</i>	CTGCGCTAAACAACACTCAACGA	GCAGATCCCTTTCAGAGCGG